

N O T I C E

THIS DOCUMENT HAS BEEN REPRODUCED FROM
MICROFICHE. ALTHOUGH IT IS RECOGNIZED THAT
CERTAIN PORTIONS ARE ILLEGIBLE, IT IS BEING RELEASED
IN THE INTEREST OF MAKING AVAILABLE AS MUCH
INFORMATION AS POSSIBLE

Contract NAS9-16055

NASA CR-160958

**BEAT FREQUENCY INTERFERENCE
PATTERN CHARACTERISTICS STUDY**

FINAL REPORT

Prepared For:

National Aeronautics and Space Administration
Lyndon B. Johnson Space Center

(NASA-CR-160958) BEAT FREQUENCY
INTERFERENCE PATTERN CHARACTERISTICS STUDY
Final Report (Novar Electronics Corp.)
102 p HC A06/MF A01

CSSL 20N

N81-25280

Unclas
63/32 26053

Prepared by:

James H. Ott
James S. Rice

January 20, 1981

Novar Electronics Corporation
24 Brown Street
Barberton, Ohio 44203



NOVAR

Contract NAS9-16055

**BEAT FREQUENCY INTERFERENCE
PATTERN CHARACTERISTICS STUDY**

FINAL REPORT

Prepared For:

**National Aeronautics and Space Administration
Lyndon B. Johnson Space Center**

Prepared by:

**James H. Ott
James S. Rice**

January 20, 1981

**Novar Electronics Corporation
24 Brown Street
Barberton, Ohio 44203**

ACKNOWLEDGEMENT

We wish to acknowledge the support and direction given by Jack Seyl and the orbital information provided by Lou Livingston, both of the NASA Johnson Space Center.

TABLE OF CONTENTS

FIGURES.vi
INTRODUCTION	1
RATIONALE	1
BACKGROUND.	1
SUMMARY OF RESULTS	3
METHODOLOGY	3
GENERAL ASSUMPTIONS	3
FREQUENCY SPECTRA OF SATELLITE SIGNALS.	6
BEAT FREQUENCIES.14
FREQUENCY SPECTRA OF BEAT FREQUENCY SIGNALS17
MITIGATING STRATEGIES21
CONCLUSIONS.29
DETAILED ANALYSIS.31
DOPPLER SHIFT31
INSTANTANEOUS POWER SPECTRAL DISTRIBUTION38
MATHEMATICAL EXPRESSION FOR THE AVERAGE POWER SPECTRAL DISTRIBUTION38
MATHEMATICAL RELATIONSHIPS AMONG THE INSTANTANEOUS AND AVERAGE POWER SPECTRAL DISTRIBUTIONS AND THE POWER SPECTRAL DENSITY.40
BEAT FREQUENCIES.42

DETAILED ANALYSIS (Continued)

BEAT FREQUENCY EXPRESSION - SINUSOIDALLY VARYING

FREQUENCIES.43

DETERMINATION OF TOTAL NUMBER OF BEAT FREQUENCY

SIGNALS.44

INSTANTANEOUS AND AVERAGE POWER SPECTRAL DISTRIBUTION

OF BEAT FREQUENCY SIGNALS.45

MITIGATING STRATEGIES.47

1. Altering the Power Beam Transmit Frequency to
Compensate for Frequency Shift at Rectenna. . . .47

a. Power Beam Frequency Shift Being Determined
by Direct or Inferential Measurement. . . .47

1.) Retrodirective Phase Control Being
Employed48

2.) Ground-Based Phase Control Being
Employed48

b. Power Beam Frequency Shift Being Determined
by Phase Conjugation With an On-Board
Atomic Clock.49

c. Evaluation of the Maximum Magnitude of the
Frequency Shift at a Point on Earth50

2. All Satellites Synchronized51

APPENDIXES

A55

I. VELOCITY OF A SATELLITE IN AN ORBIT PERTURBED

FROM GEO RELATIVE TO A POINT ON EARTH.57

II.	OPTICAL HORIZON OF THE EARTH AS SEEN FROM A SATELLITE IN GEO.65
B.	POWER SPECTRAL DENSITY OF A RECEIVED SATELLITE POWER BEAM SIGNAL67
C.	MATHEMATICAL DEVELOPMENT OF THE INSTANTANEOUS AND AVERAGE POWER SPECTRAL DISTRIBUTIONS IN TERMS OF POWER SPECTRAL DENSITY.73
D.	SPECTRAL DISTRIBUTION OF BEAT FREQUENCY SIGNALS83

FIGURES

Figure 1: Path of Satellite in Eccentric Orbit Relative to Satellite in Circular Synchronous Orbit. . . 5

Figure 2: Power Beam Frequency Variation Due to Eccentric Orbit 7

Figure 3: Typical Frequency Spectrum of 60 Satellite Power Beams at Houston - Midnight 7

Figure 4: Typical Frequency Spectrum of 60 Satellite Power Beams at Houston - 3 a.m. 7

Figure 5: Instantaneous Power Spectral Distribution in 2 Hz - Wide Contiguous Frequency Bands at Houston - Midnight. 9

Figure 6: Average of the Midnight and 3 a.m. Instantaneous Power Spectral Distributions for Houston. 9

Figure 7: Average of the Midnight, 3 a.m., 6 a.m., and 9 a.m. Instantaneous Power Spectral Distribution for Houston. 9

Figure 8: Average of 24 Instantaneous Power Spectral Distributions, One from Each Hour on the Hour, For Houston 9

Figure 9: Average Power Spectral Distribution for Houston (2 Hz - Wide Contiguous Frequency Bands) 9

Figure 10: Average Power Spectral Distribution - Houston (0.03 Hz - Wide Contiguous Frequency Bands). . .11

Figure 11: Average Power Spectral Distribution - Houston
(Expanded Frequency Scale)11

Figure 12: Average Power Spectral Distributions - Various
Locations in U.S.12

Figure 13: Average Power Spectral Distributions - Various
Locations in U.S. (Expanded Frequency Scale). .13

Figure 14: Beats Between Two Power Beam Signals Received
at Equal Power.15

Figure 15: Beat Frequency Variation Due to Variations in
Frequency of Power Beams of Two Satellites. . .16

Figure 16: Instantaneous Power Spectral Distribution at
Midnight - Barberton, Ohio.18

Figure 17: Instantaneous Power Spectral Distribution of
Beat Frequency Signals At Midnight - Barberton
Ohio.18

Figure 18: Average Power Spectral Distribution of Beat
Frequency Signals - Barberton, Ohio20

Figure 19: Average Power Spectral Distribution of Beat
Frequency Signals - Barberton, Ohio
(Logarithmic Frequency Scale)20

Figure 20: Contours of Maximum Frequency Shift on Earth
of a Power Beam Corrected for Doppler - Caused
Frequency Shift at Rectenna27

Figure 21: Geometrical Relationships Among the Earth and
Satellites in Geostationary and Eccentric
Orbits.34

**Figure A-1: Geometrical Relationships Between the Earth
and a Satellite in an Orbit Perturbed From
a Geostationary Orbit. 58**

**Figure B-1: Power Beam Frequency Variation Due to
Eccentric Orbit - "Dwell Time" in a
Frequency Band 70**

INTRODUCTION

RATIONALE

There will be relative motions between multiple Solar Power Satellites due to solar wind, lunar gravity, etc. This motion will cause beat frequency interference on the earth's surface. Although the energy of such beats would be extremely small, the frequency of these beats might cause them to be of concern.

BACKGROUND

A Solar Power Satellite moving in a geostationary orbit appears to remain fixed with respect to any point on the earth's surface. However perturbations in that orbit due to solar wind, lunar gravity, etc., will cause the satellite to be in motion relative to a point of interest on the earth and the radial component of its velocity relative to that point will cause a Doppler shift in the frequency of the energy from the power beam as observed at that point. Assuming that the Reference retrodirective phase control system is being employed wherein the satellite on-board reference phase is derived from the pilot beam, there will be an additional Doppler shift. This is due to the radial component of the satellite's velocity with respect to the pilot beam source. A multiple number of satellites in motion

relative to each other and the earth will then produce energy at a multiple number of frequencies, resulting in a very large number of beat frequencies.

SUMMARY OF RESULTS

This report presents the results of an analysis of the frequency spectra and corresponding beat frequencies created by the power beams of a multiple number of Solar Power Satellites.

METHODOLOGY

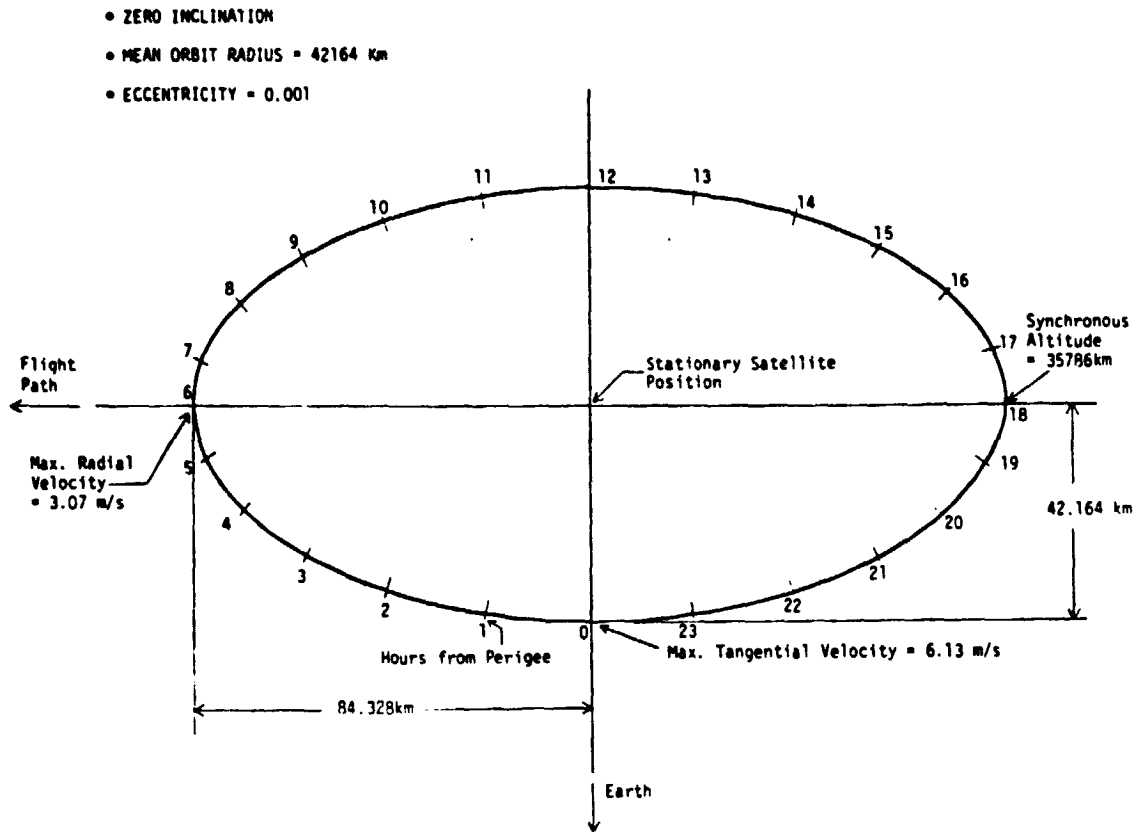
Based on the assumptions given below, the results were derived mathematically and verified through computer simulation. Frequency spectra plots were computer generated. Detailed computations were made for the seven following locations in the continental USA:

Houston, TX
Seattle, WA
Miami, FL
Chicago, IL
New York, NY
Los Angeles, CA
Barberton, OH

GENERAL ASSUMPTIONS

For the purpose of analysis, the frequency spectrum and beat frequencies created by Doppler shifts in the power beam frequencies were analyzed using the following general assumptions:

- 60 Solar Power Satellites
- Satellites located every 0.5° in longitude from 85.5° W (to 115°)
- Each satellite is in an elliptically perturbed geostationary orbit as shown in Figure 1.
 - Each orbit has an eccentricity of 0.001
 - Each orbit has zero inclination with respect to the equatorial plane. (Note: The assumptions concerning the shape and inclination of the orbits does not affect the general nature of the results of this report.)
- The specific daily times that the satellites are at the perigees of their respective orbits ("perigee times") are statistically independent random variables.
- Retrodirective phase control is used, except where otherwise noted.
- The Rectenna (pilot beam source location) for each satellite is located within $\pm 10^\circ$ longitude of that of its associated satellite.
- Equal sidelobe power is received at the seven geographical locations. (This assumption was necessary because the power at those locations is primarily a function of the power in the far sidelobes of the power beams which are undetermined at this time. Due to random phase errors, etc., at the space antennas, the far sidelobe patterns are likely to be determined primarily by the array factors of the individual power



(Information shown was supplied by NASA)

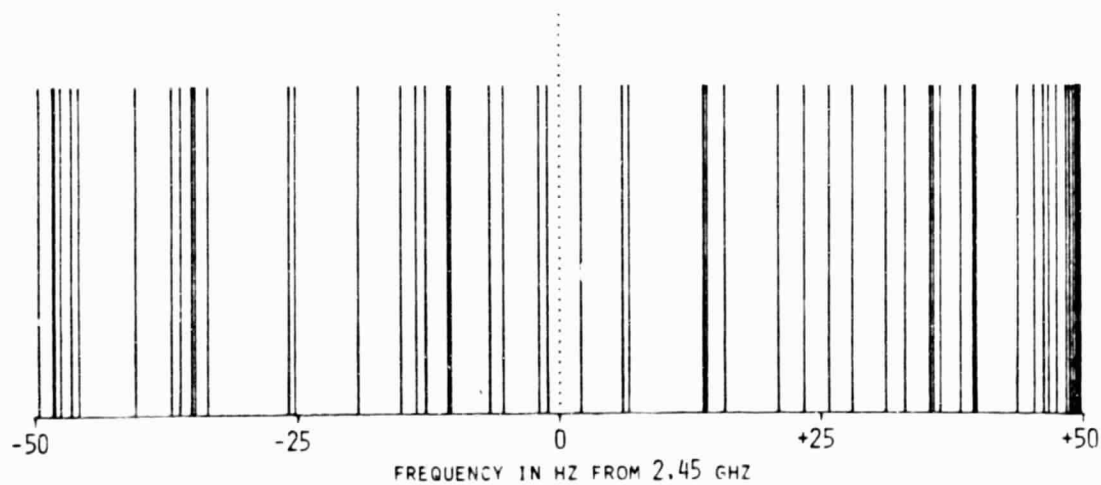
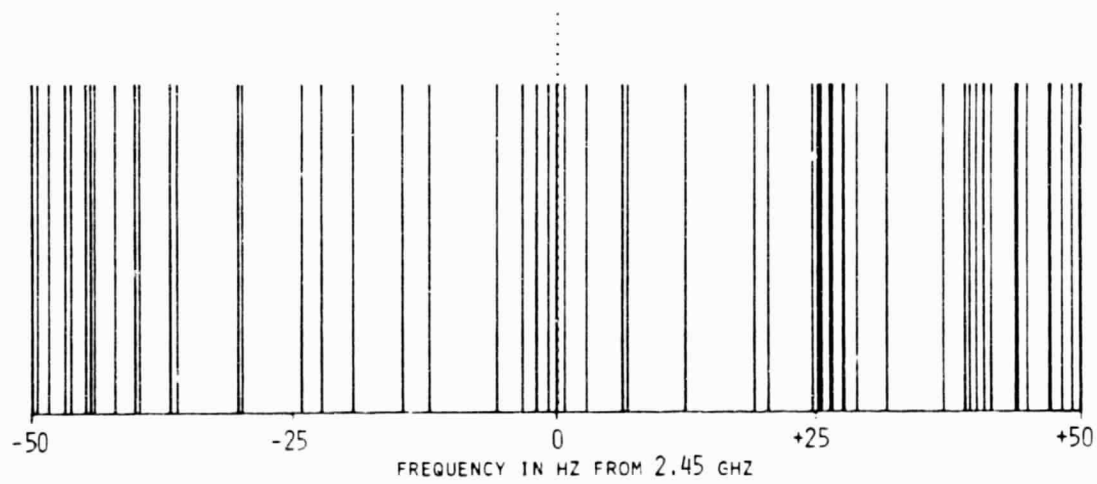
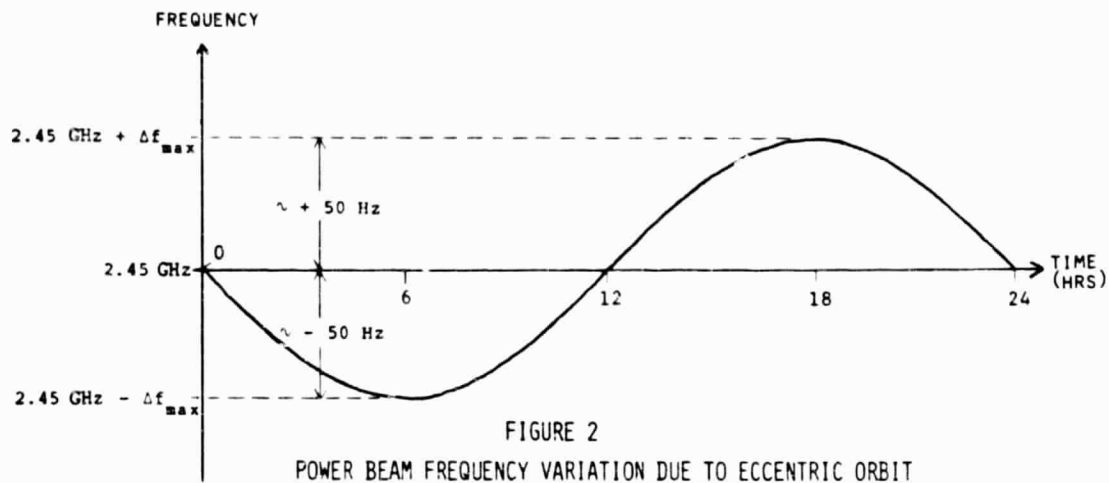
ORIGINAL PAGE IS
OF POOR QUALITY

FIGURE 1
PATH OF SATELLITE IN ECCENTRIC ORBIT RELATIVE TO
SATELLITE IN CIRCULAR SYNCHRONOUS ORBIT

modules whose broad beamwidths would cover the continental USA. As soon as specific far sidelobe antenna patterns become available, their power levels can be incorporated into the results.

FREQUENCY SPECTRA OF SATELLITE SIGNALS

The eccentric motion of a Solar Power Satellite causes a sinusoidal variation in the Doppler shift of signals transmitted to and from the satellite. The result is that the satellites's power beam signal at the earth varies sinusoidally in frequency about the intended frequency of operation. For any of the 60 satellites and seven locations selected, we show that an eccentricity of 0.001 will result in a maximum frequency deviation, Δf_{\max} , of about 50 Hz in the power beam frequency. This frequency deviation is proportional to the eccentricity. About half of the frequency deviation measured at any of the seven locations is due to the motion of the satellite with respect to its pilot beam source at the Rectenna and the remainder is due to the motion of the satellite with respect to the location studied. The period of the sinusoidal variation is 24 hours. It turns out that this result, which is shown in Figure 2, is analogous to what would result if the power beam from a satellite in geostationary orbit were frequency modulated with a sinusoidal signal whose "amplitude" and period were Δf_{\max} and 24 hours, respectively.



The 60 satellite power beams give rise to 60 signals sinusoidally varying in frequency, all with about the same maximum frequency deviation, but with random initial phases in the sinusoids of variation. A frequency spectrum that could exist in the Houston vicinity at midnight for a typical set of random perigee times is shown in Figure 3. The spectrum three hours later is shown in Figure 4.

The distribution of power in contiguous frequency bands, which we call the "Instantaneous Power Spectral Distribution (IPSD)", is shown in Figure 5 for the Houston vicinity at midnight for the perigee times used in Figures 3 and 4. The contiguous frequency bands are approximately 2 Hz wide. The IPSD is also equivalent to the percentage of frequencies that fall within each of the contiguous bands. The average of the IPSD's at midnight and 3 a.m. is shown in Figure 6. If we include in the average the IPSD's for 6 a.m. and 9 a.m. also, Figure 7 results. Including one IPSD for each hour, on the hour, starting at midnight gives the average shown in Figure 8. As more and more IPSD's are included, the average approaches the limit shown in Figure 9, which we call the "Average Power Spectral Distribution (ASPD)". An ASPD can be obtained by continuous averaging of the IPSD's over a 24 hour period. It is symmetrical about 2.45 GHz. An ASPD is equivalent to the spectral distribution that would result from 60 signals each frequency modulated by an appropriate amplitude sinewave for the case where each

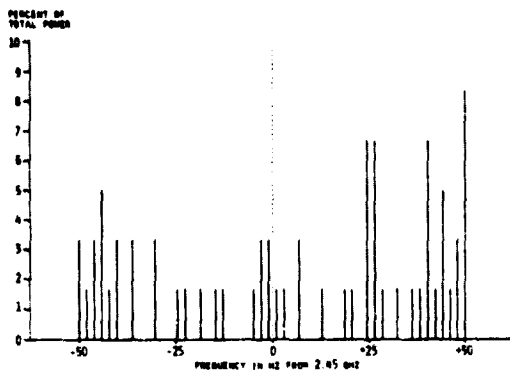


FIGURE 5
INSTANTANEOUS POWER SPECTRAL DISTRIBUTION IN 2 HZ - WIDE CONTIGUOUS FREQUENCY BANDS
AT HOUSTON - MIDNIGHT

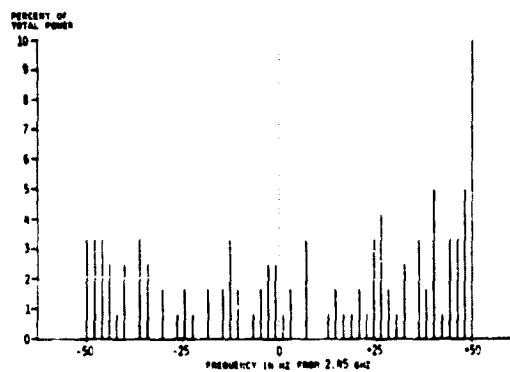


FIGURE 6
AVERAGE OF THE MIDNIGHT AND 3 A.M. INSTANTANEOUS POWER SPECTRAL DISTRIBUTIONS FOR HOUSTON

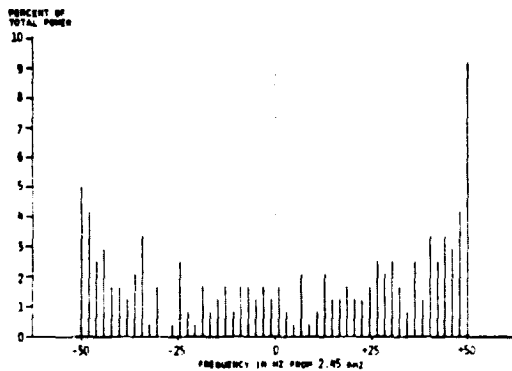


FIGURE 7
AVERAGE OF THE MIDNIGHT, 3 A.M., 6 A.M., AND 9 A.M.
INSTANTANEOUS POWER SPECTRAL DISTRIBUTIONS FOR HOUSTON

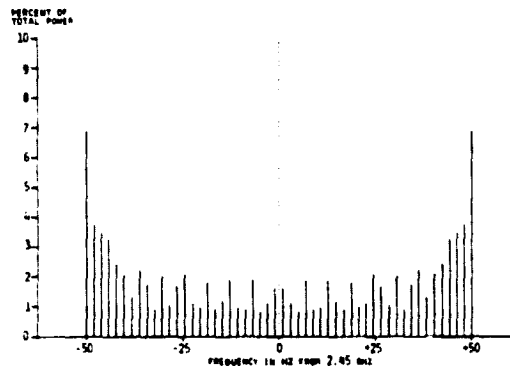


FIGURE 8
AVERAGE OF 24 INSTANTANEOUS POWER SPECTRAL DISTRIBUTIONS,
ONE FROM EACH HOUR ON THE HOUR, FOR HOUSTON

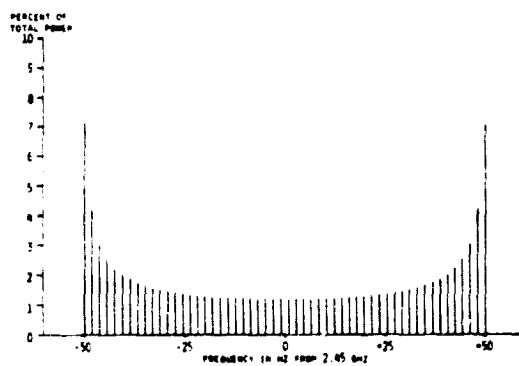


FIGURE 9
AVERAGE POWER SPECTRAL DISTRIBUTION FOR HOUSTON
(2 HZ - WIDE CONTIGUOUS FREQUENCY BANDS)

ORIGINAL PAGE 1:
OF POOR QUALITY

FIGURES 5-9

POWER SPECTRAL DISTRIBUTIONS - HOUSTON

modulation index (ratio of maximum frequency deviation to modulation frequency) is very large. Figure 10 is the same APSD as Figure 9, except that greater frequency detail in the power distribution is shown by having the contiguous frequency bands be approximately 0.03 Hz wide (as compared to approximately 2 Hz in Figures 5 through 9).^{*} Figure 11 is an expanded frequency scale version of Figure 10 to show the detail in the neighborhood of $(2.45 \times 10^9 + 50)$ Hz. APSD's for Seattle, Miami, Chicago, New York, Los Angeles, and Barberton, Ohio are shown in Figures 12 and 13.

Note that the results shown in Figures 10 through 13 are nearly identical. At each location, the average distribution in frequency of the power due to the 60 satellites is horse-shoe-shaped and is concentrated in a band approximately 100 Hz wide centered on the power beam frequency, 2.45 GHz. The reason that the APSD's are somewhat independent of the locations is that the radial velocity of a Solar Power Satellite with respect to any point in the continental USA is approximately the same. This is because the angle subtended by that portion of the earth's surface, as seen from each satellite, is small, due to the distance of the satellite from the earth compared with the earth's radius.

^{*}It is shown in the Detailed Analysis Section that the APSD is proportional to the power spectral density quantized over the contiguous frequency bands.

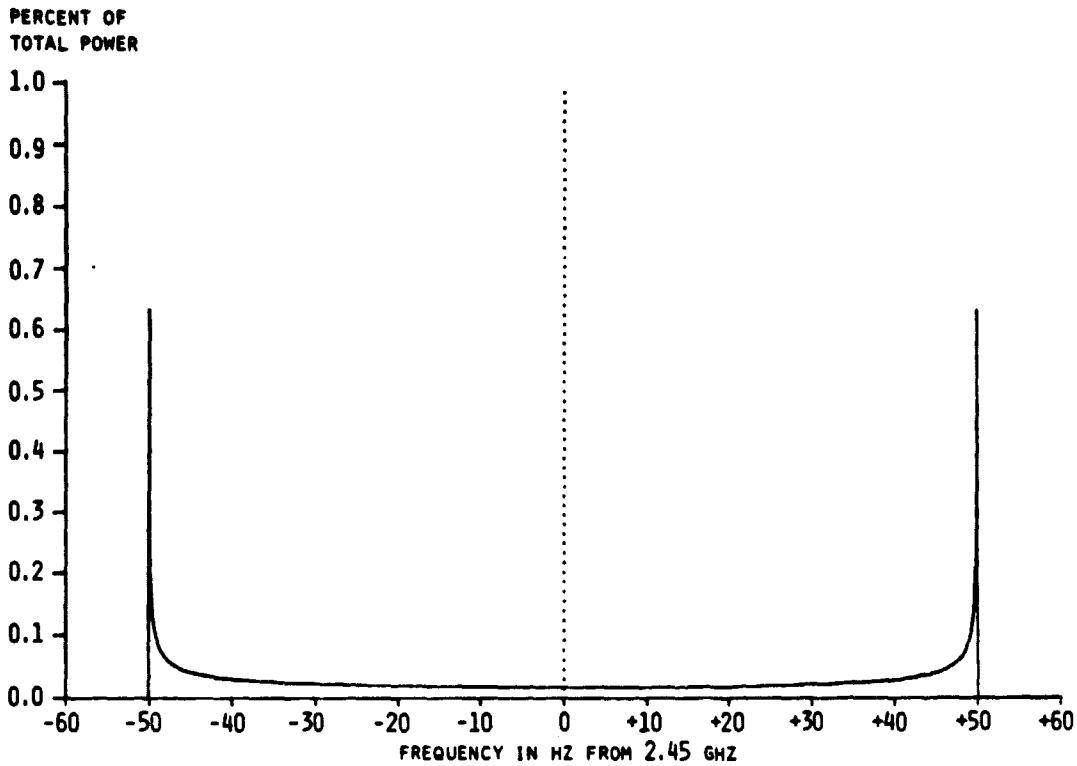


FIGURE 10
AVERAGE POWER SPECTRAL DISTRIBUTION - HOUSTON
(0.03 HZ-WIDE CONTIGUOUS FREQUENCY BANDS)

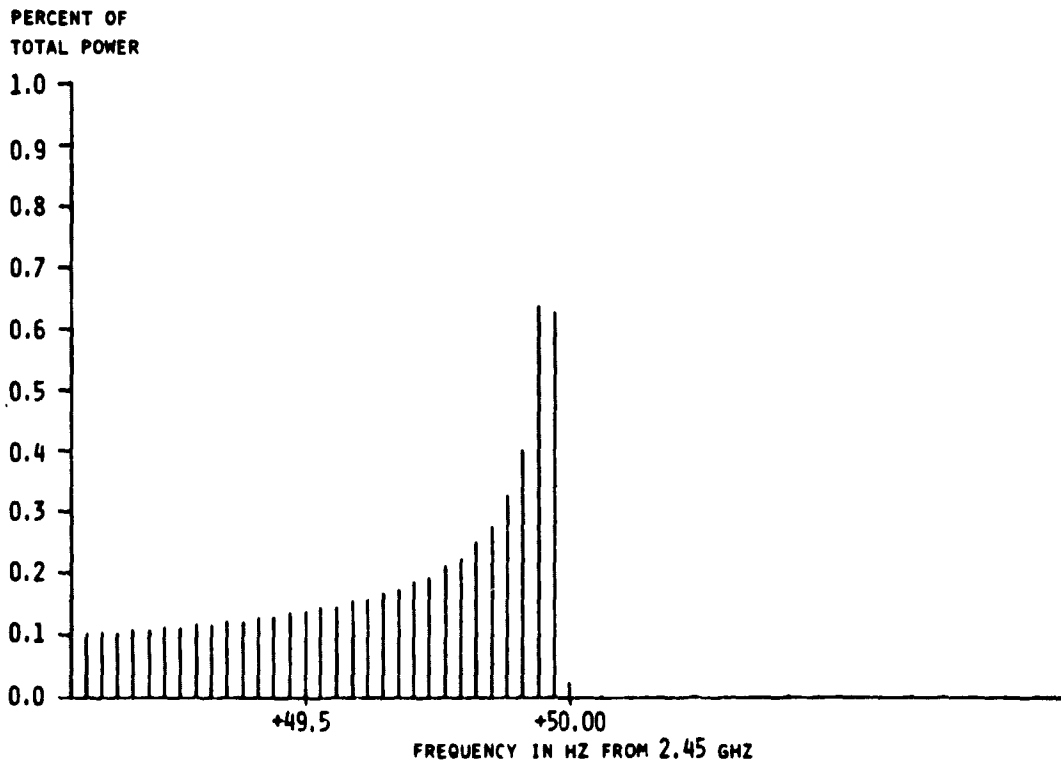
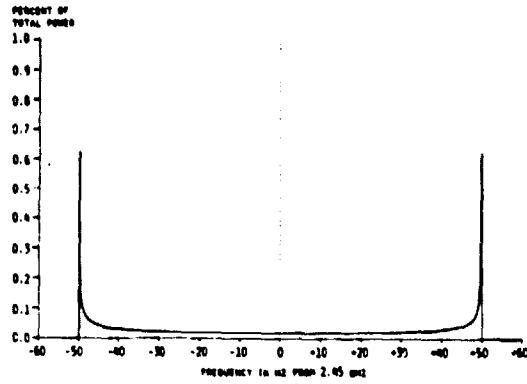
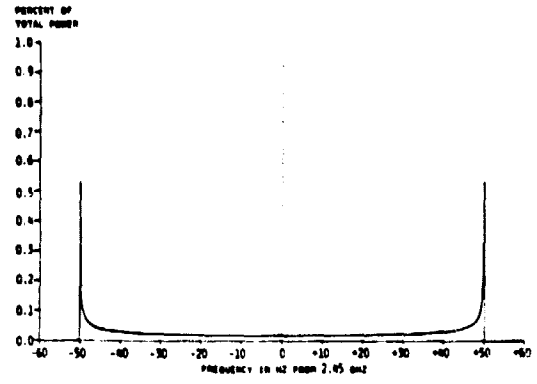


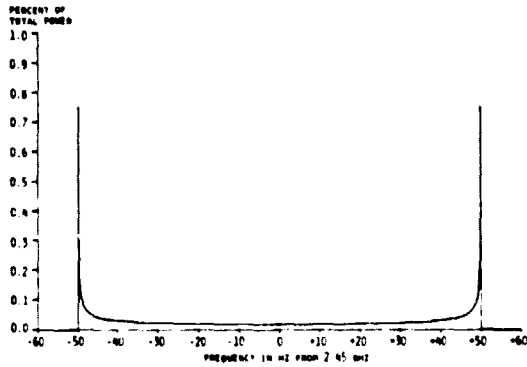
FIGURE 11
AVERAGE POWER SPECTRAL DISTRIBUTION - HOUSTON
(EXPANDED FREQUENCY SCALE, 2.45 GHZ + 50 HZ REGION)



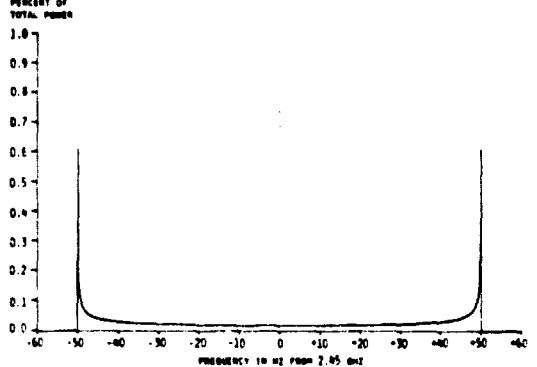
(a)
SEATTLE



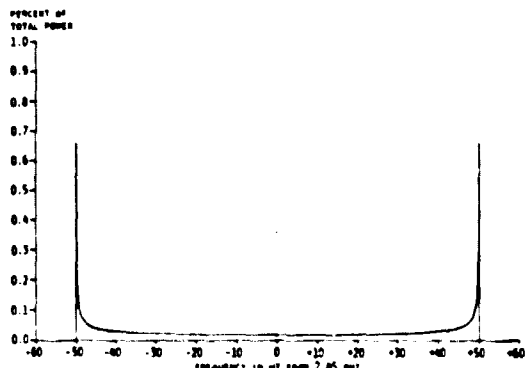
(b)
MIAMI



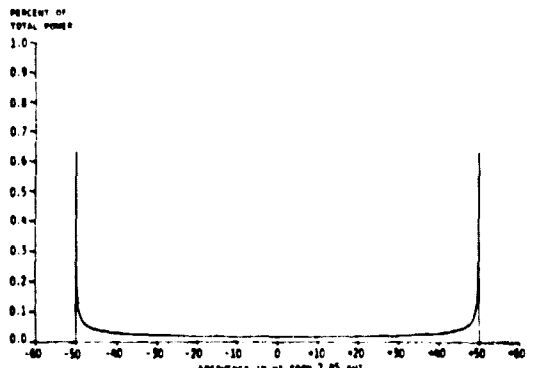
(c)
CHICAGO



(d)
NEW YORK

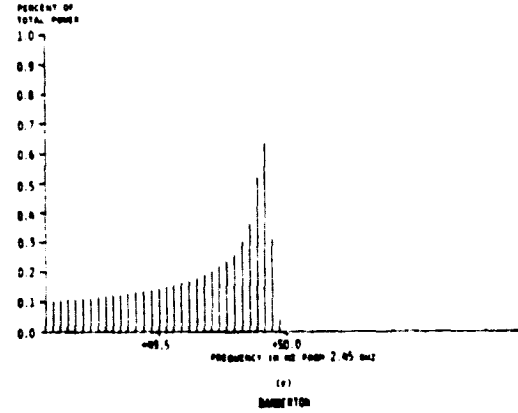
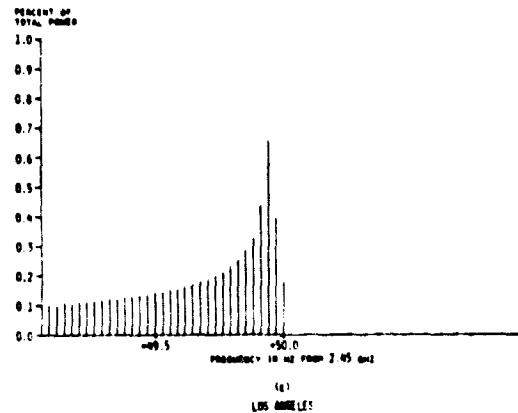
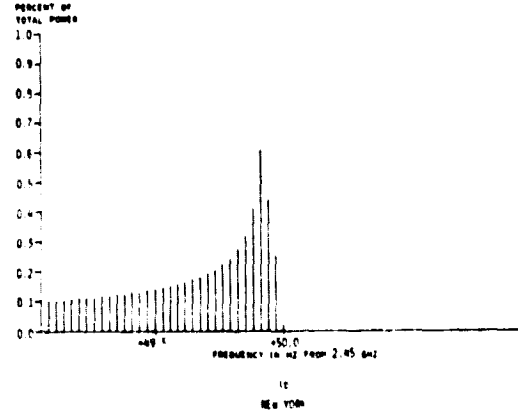
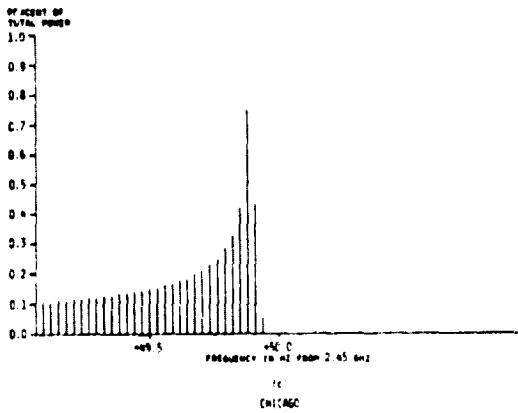
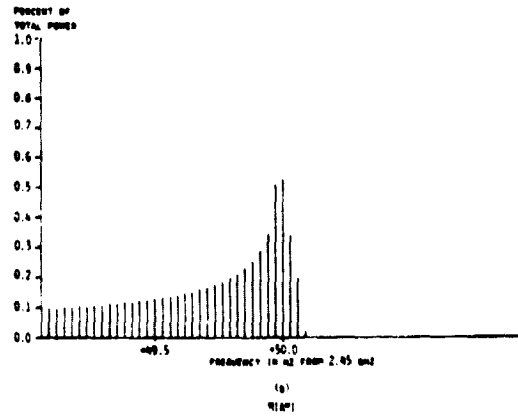
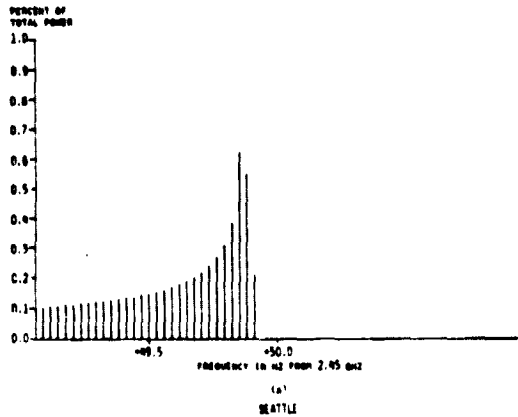


(e)
LOS ANGELES



(f)
SAN ANTONIO

FIGURE 12
AVERAGE POWER SPECTRAL DISTRIBUTIONS - VARIOUS LOCATIONS IN U.S.



ORIGINAL PAGE IS
OF POOR QUALITY

FIGURE 13

AVERAGE POWER SPECTRAL DISTRIBUTIONS - VARIOUS LOCATIONS IN U.S.
(EXPANDED FREQUENCY SCALE)

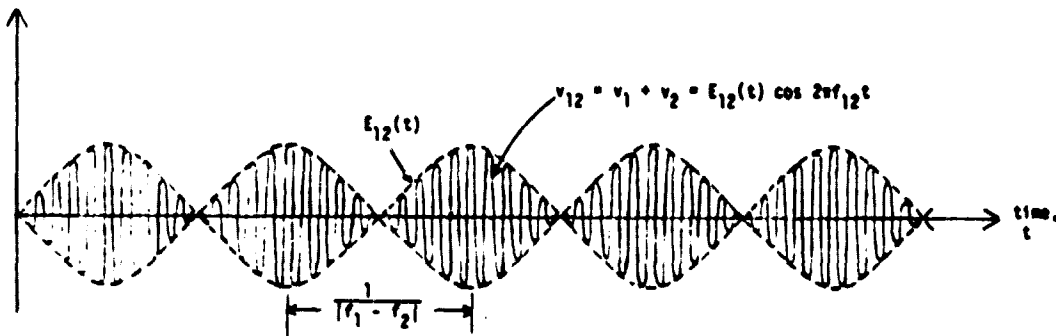
BEAT FREQUENCIES

The sum of two signals forms a composite signal whose maximum amplitude fluctuates ("beats") at a rate equal to the difference in the frequencies of the two signals (the "beat frequency"). This is shown in Figure 14 for the case of two signals of equal power, where f_1 and f_2 are the instantaneous frequencies of the two signals, and $|f_1 - f_2|$ is the instantaneous beat frequency. Thus power beam signals differing in frequency at the earth's surface due to differences in Doppler shifts will generate beat frequencies.

Since the frequencies of the satellite power beams each vary sinusoidally with time, the beat frequency due to any two satellites varies with time over a frequency range from zero to some maximum frequency, with the period of the beat frequency variation being 12 hours. The maximum beat frequency can be from near zero to approximately 100 Hz depending primarily on the respective initial phase of the sinusoids of variation in the two power beam frequencies. Figure 15 illustrates two cases. For 60 satellites, there are almost 1800 possible beat frequencies at any time.

It is essential to recognize in Figure 14 that there is actually no signal at the beat frequency or at any other frequency except f_1 and f_2 , the instantaneous frequencies of the original two signals. The mere addition of two signals varying sinusoidally in amplitude at two different frequencies

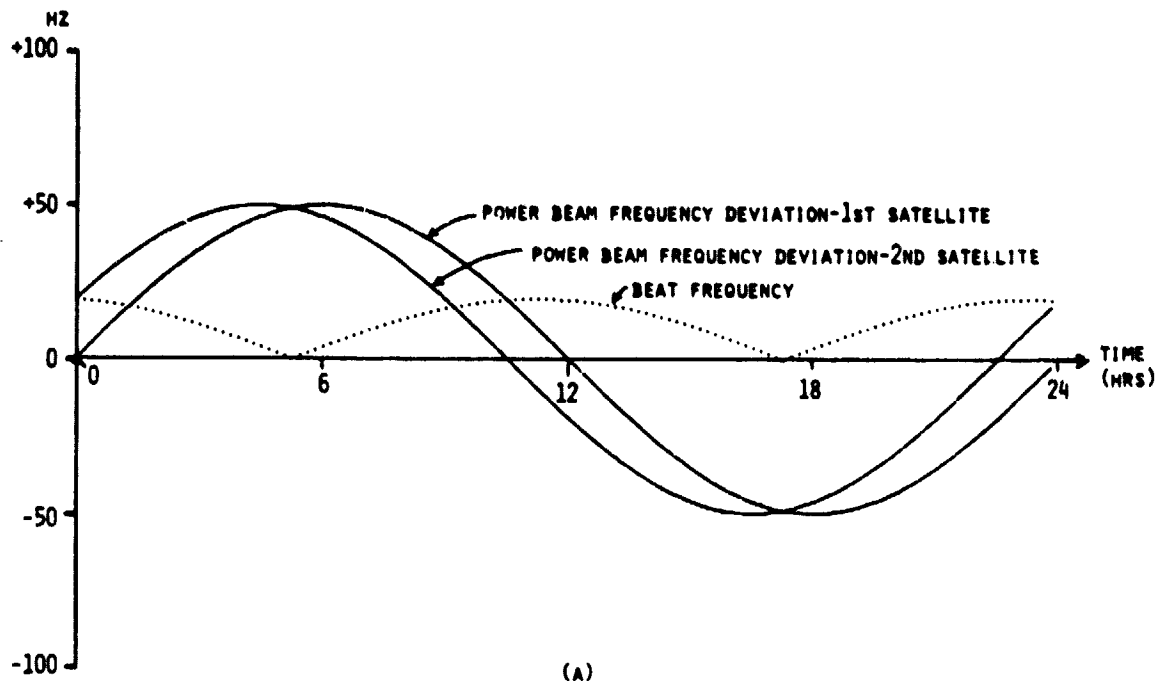
Amplitude of Composite Signal, v_{12}



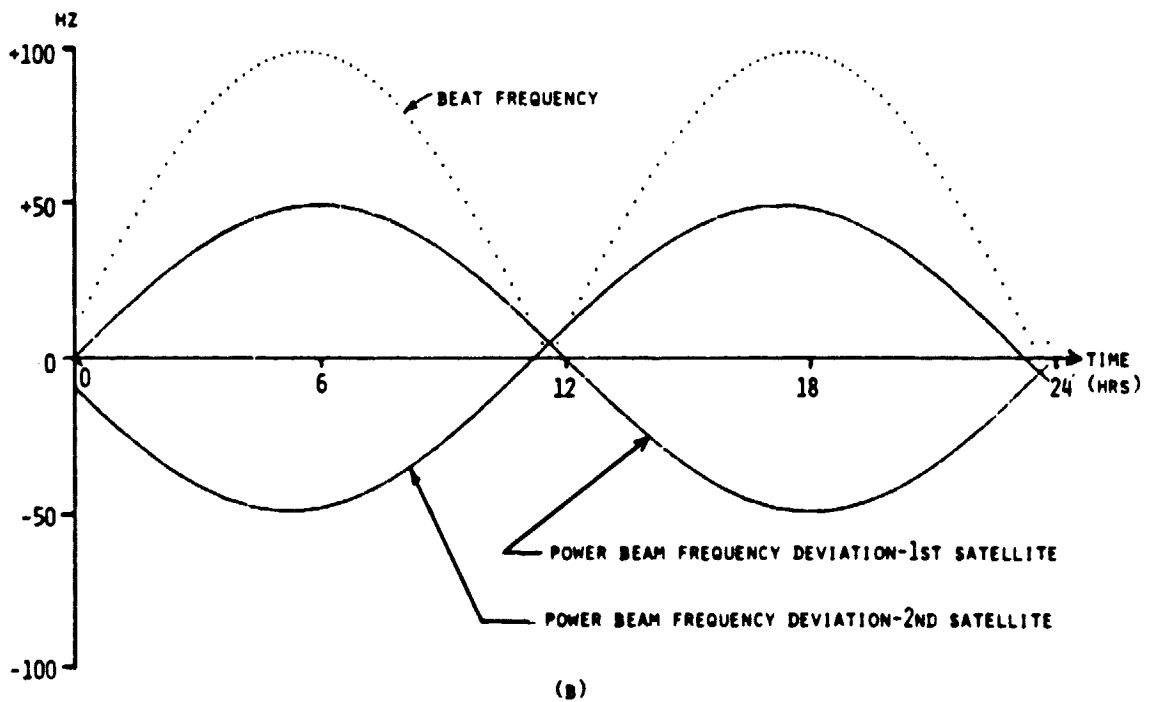
- v_1 and v_2 are two power beam signals of equal amplitude (power) with instantaneous frequencies f_1 and f_2 .
- $E_{12}(t)$ is the envelope of the maximum amplitude of the composite signal.
- f_{12} is the geometric mean of f_1 and f_2 .
- $|f_1 - f_2|$ is the beat frequency.

FIGURE 14

BEATS BETWEEN TWO POWER BEAM SIGNALS RECEIVED WITH EQUAL POWER



(A)
POWER BEAM FREQUENCY VARIATIONS NEARLY "IN PHASE"



(B)
POWER BEAM FREQUENCY VARIATIONS NEARLY "OUT OF PHASE"

FIGURE 15
BEAT FREQUENCY VARIATION DUE TO VARIATIONS IN FREQUENCY OF
POWER BEAMS OF TWO SATELLITES

cannot create a signal at a new frequency. Signals at the beat frequency can only be obtained through distortion of the waveform (of the two additive signals) by some non-linear process. One such process is thermal heating, which is proportional to the square of the instantaneous amplitude of the signal shown in Figure 14, and produces energy at the frequency $|f_1 - f_2|$. Any non-linearity which causes the generation of the product of two signals will produce a beat frequency signal. A non-linear process which squares the composite (the sum) of the two signals does this--a "square-law" non-linearity. For the purposes of this report, then, we assume that any non-linear process present is square-law. A square-law process is not only very reasonable to expect, but also one that allows us to conveniently calculate and look at the power spectrum of the beat frequency signals--the Instantaneous and the Average Power Spectral Distributions of the beat frequency signals ($IPSD_B$ and $APSD_B$).

FREQUENCY SPECTRA OF BEAT FREQUENCY SIGNALS

Consider a possible frequency spectrum for the 60 satellite power beams received, for example, at Barberton, Ohio at midnight. This is shown in Figure 16. For equal power received from all 60 satellites, and for 0.024 Hz-wide contiguous frequency bands, Figure 16 then represents the $IPSD$ at midnight for Barberton. These 60 satellite signals generate almost 1800 beat frequency signals. Figure 17 shows the frequency distribution of power for the beat frequency

FRACTION OF
TOTAL POWER

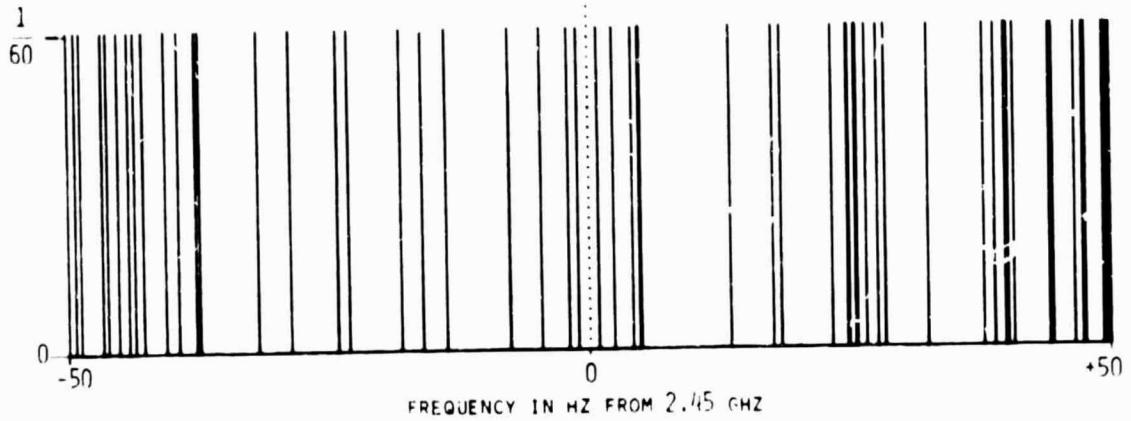


FIGURE 16
INSTANTANEOUS POWER SPECTRAL DISTRIBUTION AT MIDNIGHT - BARBERTON, OHIO
(0.024HZ-WIDE CONTIGUOUS FREQUENCY BANDS)

PERCENT OF
TOTAL POWER

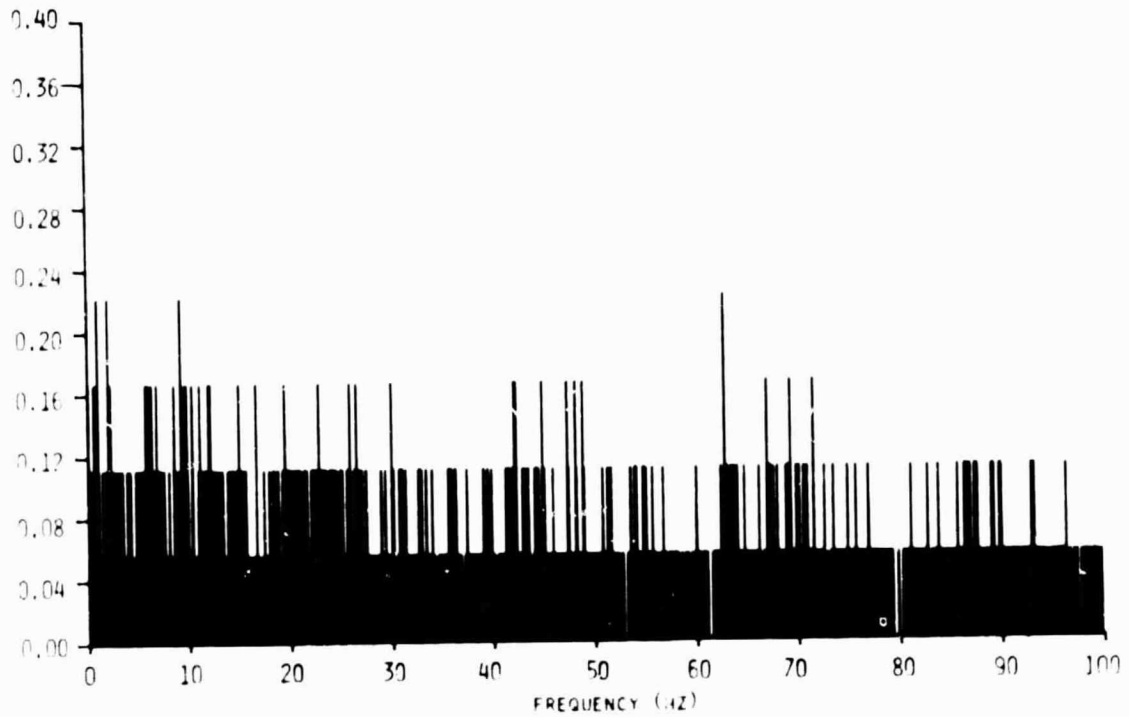


FIGURE 17
INSTANTANEOUS POWER SPECTRAL DISTRIBUTION OF BEAT FREQUENCY SIGNALS
AT MIDNIGHT - BARBERTON, OHIO
(0.024HZ-WIDE CONTIGUOUS FREQUENCY BANDS)

ORIGINAL PAGE IS
OF POOR QUALITY

signals in narrow contiguous frequency bands--the Instantaneous Power Spectral Distribution of the beat frequency signals ($IPSD_B$) at midnight for Barberton, Ohio. The beat frequencies extend almost to 100 Hz. Figure 17 also represents the percentage of beat frequencies that fall within each of the contiguous bands.

Since the time of day that each satellite is at its perigee is assumed to be a random variable, the power spectral distribution at any time can be expected to average out to be as shown in Figure 18--the Average Power Spectral Distribution of the beat frequency signals ($APSD_B$) for Barberton, Ohio. The maximum frequency is approximately 100 Hz and the contiguous frequency bands are 0.03 Hz wide. Figure 19 shows that the $APSD_B$ of Figure 18 is almost a linear function when plotted with a logarithmic frequency scale.

The $APSD_B$, as shown in Figure 18 and 19, is the statistical average (statistical expectation) of the $IPSD_B$, and is not necessarily the same as the 24-hour time average. However, the time average of the $IPSD_B$'s should be very close to the $APSD_B$.

Figure 18 and 19, are for all practical purposes, representative of the plots of an $APSD_B$ at any location in the continental U.S.A.

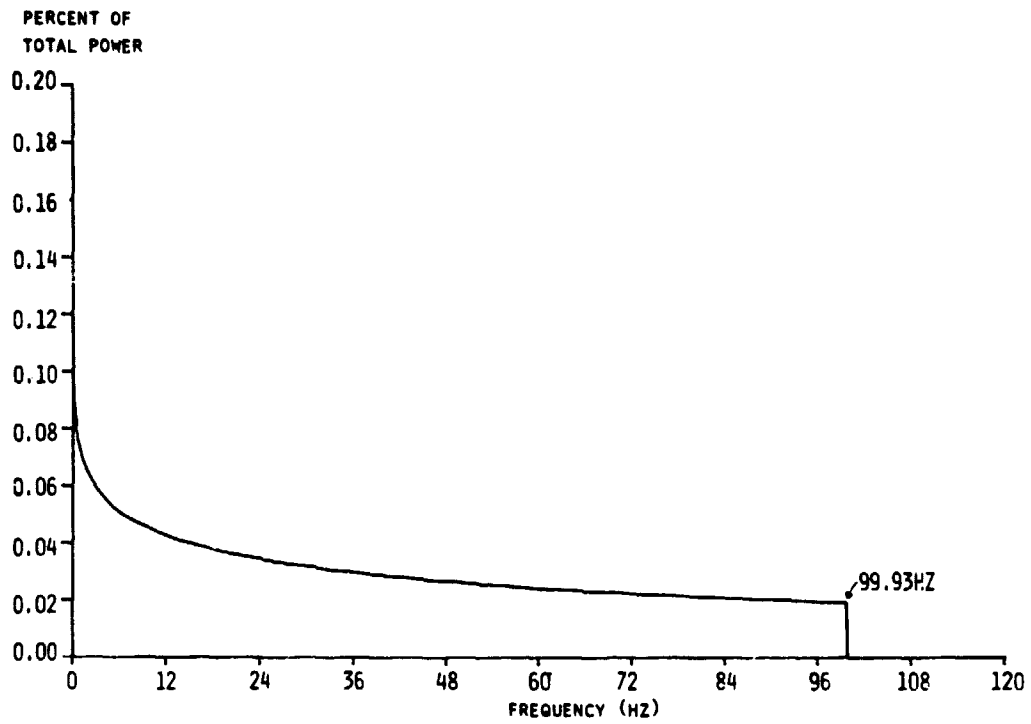


FIGURE 18
 AVERAGE POWER SPECTRAL DISTRIBUTION OF BEAT FREQUENCY SIGNALS
 -BARBERTON, OHIO
 (0.03HZ-WIDE CONTIGUOUS FREQUENCY BANDS)

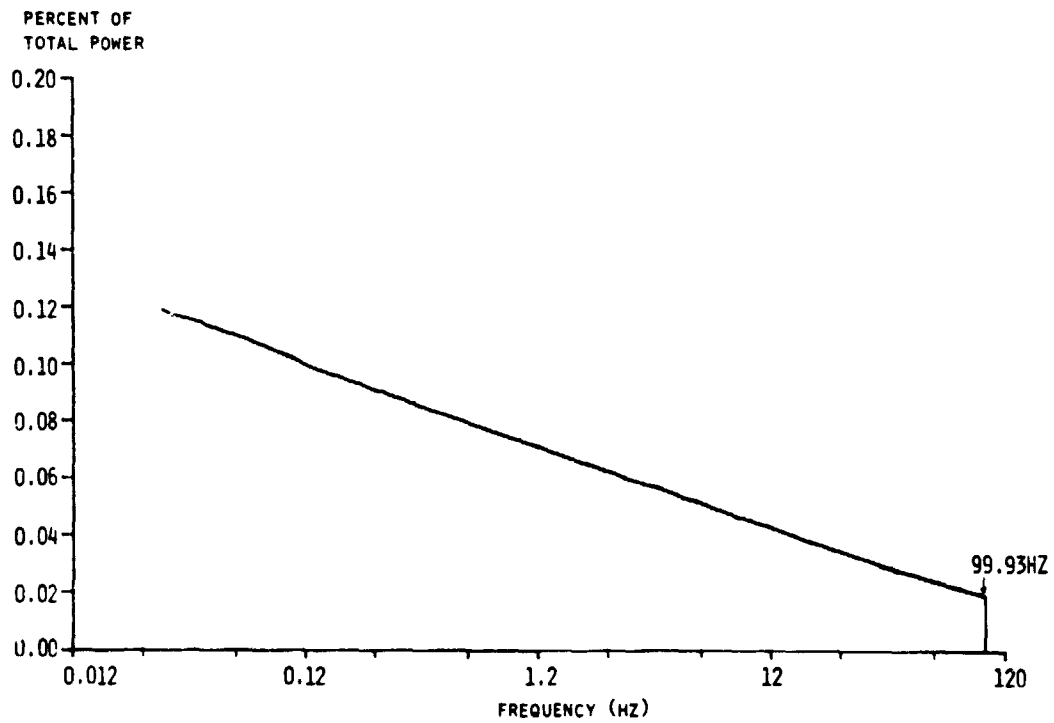


FIGURE 19
 AVERAGE POWER SPECTRAL DISTRIBUTION OF BEAT FREQUENCY SIGNALS
 -BARBERTON, OHIO
 (LOGARITHMIC FREQUENCY SCALE)

MITIGATING STRATEGIES

Separate Transmit Frequencies For Each SPS

The beat frequencies that have been discussed so far are from retrodirective phase controlled satellites transmitting at nominally the same frequency and fall within the frequency range from zero to 100 Hz or so. By purposely separating the transmit frequencies of the power beams, the beat frequencies can all be made to fall above the zero to 100 Hz range because the minimum beat frequency will be the minimum frequency difference between any two power beams. However, to avoid any pumping in the ionosphere, that is, to avoid generating RFI due to the non-linear action of the ionosphere on microwave signals differing in frequency, the power beam frequency separation must be on the order of 100 MHz. Therefore for a large number of power satellites we would run out of spectrum for the transmitting frequencies.

All Transmit Frequencies Nominally the Same

Since the beat frequencies for power satellites all transmitting at nominally the same frequency are caused by differences in Doppler shifts, several mitigating strategies were investigated which minimize the differences or minimize the effects of the differences. These strategies fall into two categories--stationkeeping techniques and techniques that alter the transmit frequency of the power beat at the satellite.

Stationkeeping - Maintain Satellites in Nearly Exact GEO

One obvious stationkeeping technique is to keep all satellites exactly or nearly exactly in GEO to essentially eliminate any relative motion of the satellites. Since a satellite's relative velocity is proportional to orbit eccentricity, then the Doppler shifts will be also. This means that since the maximum possible beat frequency is approximately 100 Hz (from Figure 18 and 19) for orbit eccentricities of 0.001, the orbit eccentricities would have to be an order of magnitude better (less than 0.0001) to keep the maximum possible beat frequency to under 10 Hz. This technique is probably not practical and probably would require an excessive amount of fuel for stationkeeping.

Stationkeeping - Synchronized Satellites

A second stationkeeping technique allows for eccentric orbits, but requires that the orbit inclinations and eccentricities be identical and that the satellites be synchronized in such a manner that the magnitude and "phase" of the perturbations from GEO for each be identical at all times. This is equivalent to saying that at any time all satellites will be at the same relative point in orbits identically perturbed from GEO. Since the velocities of the satellites towards the center of the earth would therefore be identical at all times, the Doppler shifts at any point on earth due to the motion of the satellites will tend to be the same and

will thereby tend to cancel out frequency differences. For the general assumptions of this report, namely zero orbit inclination, all eccentricities equal to 0.001, and satellites located over a longitudinal span of approximately 30° from 85.5° to 115° , the maximum beat frequency on earth will be under 5 Hz. Whether this stationkeeping technique is even feasible is another question.

Transmit Frequency Altering Techniques

Techniques that alter the transmit frequency of the power beam at the satellite do so in order to compensate for the frequency shift at earth caused by Doppler shift.

Transmit Frequency Alteration - Determined by Frequency Shift at Rectenna

One transmit frequency altering technique shifts the transmit frequency at the satellite by an amount equal to the frequency shift measured at the Rectenna, that is, by an amount equal to the difference from 2.45 GHz in the frequency of the received power beam.* If a retrodirective phase control

* Note that the 2.45 GHz reference source at each Rectenna, even if only used to determine the pilot beam frequency of satellites that are "perfectly" in GEO and hence have no relative motions, must be calibrated or referenced to some common frequency source so as to have a frequency difference less than 10 Hz. If the maximum compensated frequency

system is being employed, the satellite transmit frequency is shifted by shifting the pilot beam frequency by the measured frequency shift at the Rectenna. If a ground-based phase control system is being employed, such as Interferometer-Based Phase Control^{*}, the transmit frequency at the satellite can be changed in one of two ways as a result of the measurement of the frequency shift at the Rectenna. It can be changed via a command link or can be frequency-locked to a frequency which is synthesized from a pilot signal transmitted to the satellite at some suitable frequency, say $\frac{1}{2} \times 2.45$ GHz. In this case, the pilot signal frequency is compensated by the power beam frequency shift measured at the Rectenna.

The power beam frequency shift at the Rectenna can be measured by direct comparison of the power beam frequency with a local oscillator at 2.45 GHz. The power beam frequency measurement/correction loop only needs to operate very slowly. difference between satellites due to any mitigating strategy is, say 10 Hz, then the reference sources might have to be, say, within 1 Hz!

*J. H. Ott and J. S. Rice "An Interferometer-Based Phase Control System", Final Proceedings of the Solar Power Satellite Program Review, Lincoln, Nebraska, April 22-25, 1980, pp. 289-292. (Available from National Technical Information Service.)

This allows long measurement integration times for highly accurate determination of the frequency shift at the Rectenna. The slow operation of the loop is allowed by the low rate of change in the Doppler-caused frequency shift in the received power beam which is at most on the order of one Hertz per minute.

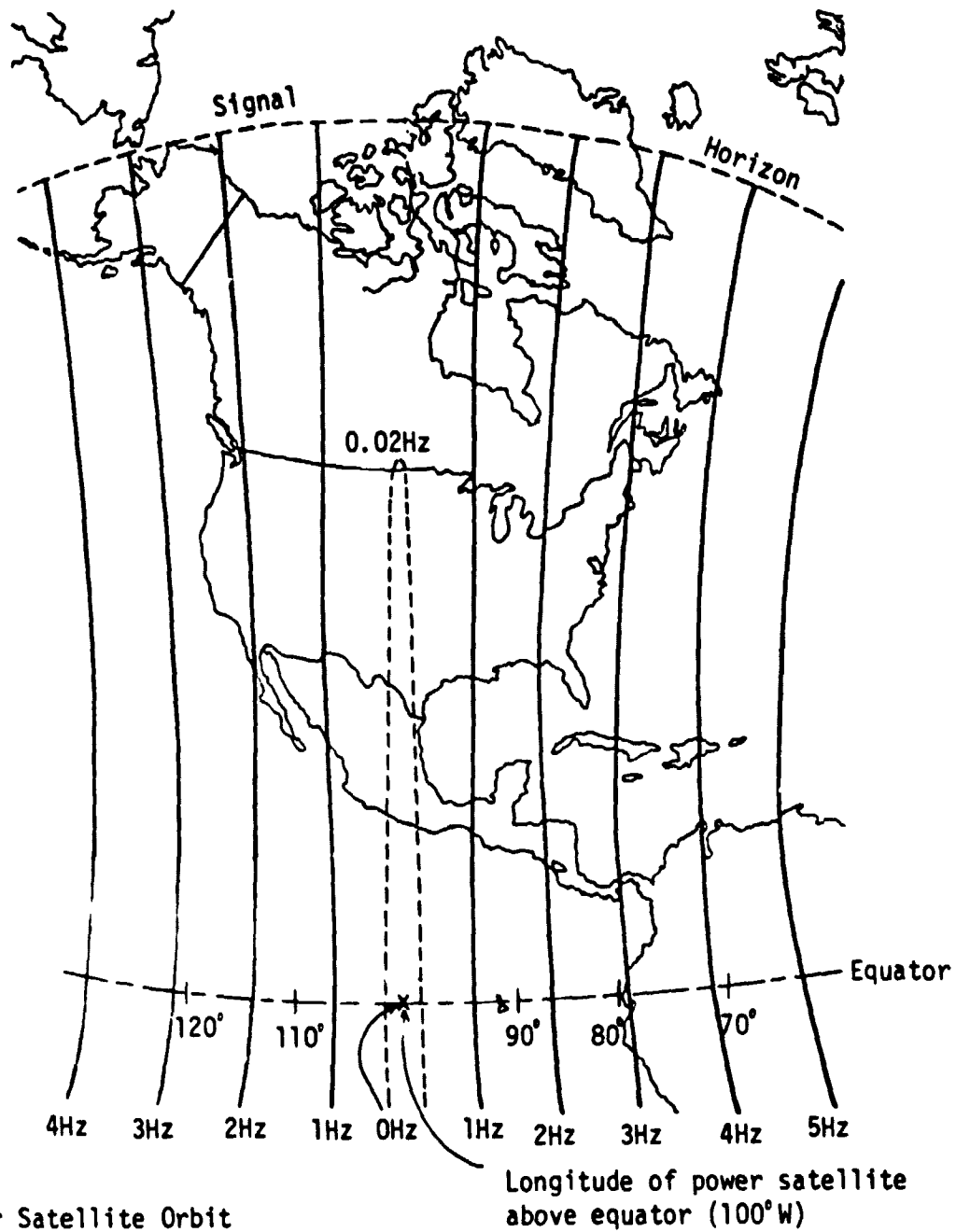
For correction purposes, it may not even be necessary to directly measure the power beam frequency shift on earth but only to infer it. The power beam transmit frequency can be altered in a predictive fashion just by knowledge of the orbital characteristics. The power beam frequency shift at the Rectenna is a sinusoidal function of time, with the maximum magnitude of the shift being proportional to eccentricity. The shift is zero when the satellite is at its apogee and perigee, and is at its positive and negative maximums 6 hours respectively from the time it is at its apogee and perigee.

Transmit Frequency Alteration - By Means of On-Board Atomic Clock

Another transmit frequency altering technique uses an on-board atomic clock at each satellite to generate a reference signal at a frequency of 2×2.45 GHz. When retrodirective phase control is being employed, the 4.9 GHz reference signal would be used as the reference signal for the phase conjugation of the received pilot beam. Thus the phase con-

jugation process would automatically shift the power beam frequency by a compensating amount equal to the Doppler shift between the pilot beam source (the Rectenna) and the satellite. If ground based phase control is being employed, an uplink signal from the Rectenna would serve the same purpose as that served by the pilot beam in retrodirective phase control for generation of the power beam transmit frequency.

All of the mentioned techniques that alter the transmit frequency of the power beam in a compensating manner result in a perfectly corrected frequency shift only at the Rectenna. The corrected frequency shift any place else is strictly a function of the geographical location of that place. Figure 20 is a geographical plot of the contours of corrected frequency shift for a satellite located at longitude 100° W. These are maximum magnitude contours. For a satellite located at other than 100° W, the contours change longitude by an amount equal to the difference between 100° W and the longitude of the satellite. To find the maximum possible beat frequency between two satellites, assume that the two satellites are located in their respective orbits such that at a geographical point of interest, one satellite's corrected frequency shift is at its positive maximum when the other is at its negative maximum. The maximum possible beat frequency is then just the sum of the frequencies of



Power Satellite Orbit
 Characteristics:
 Zero Inclination
 Eccentricity = 0.001

Longitude of power satellite
 above equator (100° W)

ORIGINAL PAGE IS
 OF POOR QUALITY

FIGURE 20

CONTOURS OF MAXIMUM FREQUENCY SHIFT ON EARTH OF A POWER BEAM CORRECTED
 FOR DOPPLER-CAUSED FREQUENCY SHIFTS AT RECTENNA
 (Magnitude, in Hz, from 2.45GHz)

the two contours which exist at that point from the two satellites. From inspection of the contours of Figure 20, it can be determined that the maximum beat frequency that is possible (i.e., worst case) in the continental U.S.A. due to two satellites located anywhere from longitude 85.5° W to 115° W is about 9 Hz.

CONCLUSIONS

Power satellites in orbits spanning 30° of longitude about longitude 100° W will generate beat frequencies from zero to a maximum frequency which is proportional to orbital eccentricity (all eccentricities equal), and roughly proportional to the maximum eccentricity present (eccentricities unequal). In the continental U.S.A., for the above placed satellites:

1. Eccentricities all equal to 0.001 can result in beat frequencies from 0 to 100 Hz for retrodirective phase control systems. Maximum beat frequency will be under 10 Hz for eccentricities less than 0.0001.
2. Mitigating strategies have been determined which which maintain the maximum possible beat frequency to under 10 Hz for eccentricities up to 0.001 (maximum possible beat frequency roughly proportional to maximum eccentricity present).

DETAILED ANALYSIS

DOPPLER SHIFT

The Doppler shift in the power beam frequency of a Solar Power Satellite as observed at a point P_E , on the earth's surface, relative to the frequency transmitted by the satellite, is given by the expression

$$(1) \quad \Delta f = - f \frac{v}{c}$$

where Δf is the observed frequency shift, f is the frequency transmitted by the satellite, c is the velocity of light, and v is the radial velocity of the satellite with respect to P_E in a direction away from P_E . Equation 1 also expresses the Doppler shift in the frequency of the pilot beam as received at the satellite, with P_E representing the location of the pilot beam source (center of Rectenna), and f the transmitted frequency of the pilot beam. Both v and c remain defined as before. The v which corresponds to the P_E of concern is given by Equation 2. This is derived in Appendix A based on the geometry of the situation, with the symbols as defined in Figure A-1.

PRECEDING PAGE BLANK NOT FILMED

$$(2) \quad v = \frac{\begin{bmatrix} v_R [(r_G + \Delta x) - r_E \cos \phi \cos \Delta \theta] \\ + v_T [\Delta y - r_E \cos \phi \sin \theta] \\ + v_N [\Delta z - r_E \sin \theta] \end{bmatrix}}{\sqrt{(r_G + \Delta x)^2 + \Delta y^2 + \Delta z^2 + r_E^2 - 2r_E \{ [(r_G + \Delta x) \cos \Delta \theta + \Delta y \sin \Delta \theta] \cos \phi + \Delta z \sin \phi \}}}$$

For a zero inclined elliptical orbit with eccentricity equal to 0.001, Δz and the numerator term involving v_N are zero, and Δx and Δy^* can be neglected with a resulting maximum error on the order of only about 0.1 Hz in the Doppler shift. This is equivalent to ignoring the perturbation in the position of the satellite from exact ideal GEO. Equation 2 then simplifies to the following:

$$v = \frac{v_R \left(1 - \frac{r_E}{r_G} \cos \phi \cos \Delta \theta\right) - v_T \left(\frac{r_E}{r_G} \cos \phi \sin \Delta \theta\right)}{\sqrt{1 + \left(\frac{r_E}{r_G}\right)^2 - 2 \frac{r_E}{r_G} \cos \phi \cos \Delta \theta}}$$

Figure 21 depicts the situation. From Appendix A, numerical expressions for v_R and v_T are given by:

$$(4a) \quad v_R = 3.07 \sin \frac{2\pi}{T} t \text{ (meters/sec.)}$$

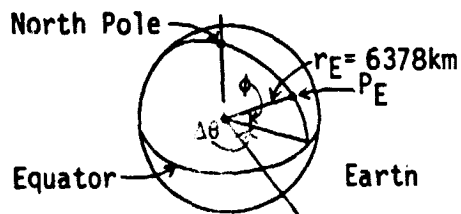
$$(4b) \quad v_T = 6.13 \cos \frac{2\pi}{T} t \text{ (meters/sec.)}$$

*Figure 1 shows that Δx and Δy have maximum values of 42 km and 84 km, respectively.

where t is the time, in hours, of the satellite from its perigee, and $T = 24$ hours. v_R and v_T are proportional to the eccentricity.

It was assumed that a Rectenna site (pilot beam transmitter location) is within $\pm 10^\circ$ longitude of its corresponding power satellite. Thus $|\Delta\theta| \leq 10^\circ$, and the Doppler shift in the received pilot beam frequency at the satellite can be approximated by letting $v = v_R$ in Equation 1. This is equivalent to $\phi = 0$, and $\Delta\theta = 0$ in Equation 3, which for calculation purposes, puts the pilot beam transmitter on the equator at the same longitude as the satellite. A more accurate expression for this v would be obtained by continuing to let $\Delta\theta = 0$ in Equation 3 and letting ϕ equal some mean latitude of all the Rectennas. However, the maximum error in the Doppler shift using $v = v_R$ was determined by calculation to be only on the order of about 0.1 Hz, and therefore v_R is used in this report for the Doppler shift in the pilot beam frequency.

Let f_0 be the transmitted frequency of the pilot beam, f_1 be that of the power beam at the satellite, and v_R and v_{SE} be the velocities of the satellite with respect to its associated Rectenna (pilot beam transmitter), and with respect to P_E , a location of interest on earth. The frequency shift, Δf_e , observed at P_E relative to f_0 , due to Doppler shifts, is then given by



(Symbols defined on next page.)

$r_G = 42164\text{km}$

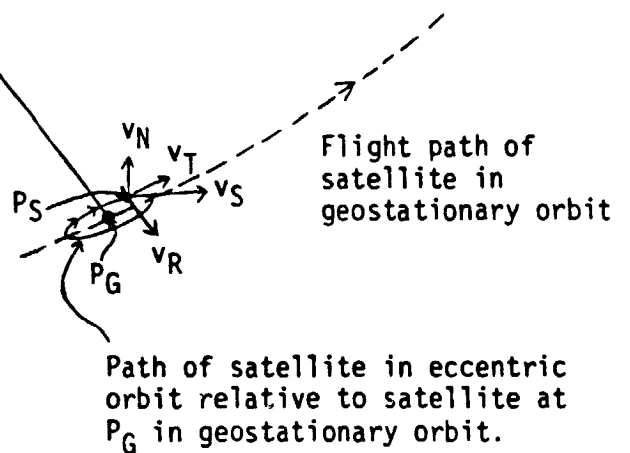


FIGURE 21

GEOMETRICAL RELATIONSHIPS AMONG THE EARTH AND SATELLITES IN GEOSTATIONARY AND ECCENTRIC ORBITS

DEFINITIONS OF SYMBOLS

- P_E = arbitrary point on the earth's surface
 P_S = instantaneous position of satellite relative to P_E
 P_G = mean position of satellite relative to P_E , equal to position of a satellite in geostationary orbit relative to P_E
 ϕ = latitude of P_E (ϕ is positive in northern hemisphere)
 $\Delta\theta$ = longitudinal difference between P_G and P_E . ($\Delta\theta$ is positive if P_G is west of P_E)
 v_S = instantaneous satellite velocity relative to P_G
 $v_S = \sqrt{v_R^2 + v_T^2 + v_N^2}$, where v_R, v_T, v_N are corresponding orthogonal components of v_S with directions defined as follows:
 v_R : radially away from center of earth
 v_T : direction of flight of geostationary satellite at P_G
 v_N : normal to equatorial plane (toward North Star)
 r_E = radius of earth
 r_G = radius of geostationary orbit
 d = distance between P_S and P_G (positional variation of P_S with respect to P_G)
 $d = \sqrt{(\Delta x)^2 + (\Delta y)^2 + (\Delta z)^2}$, where $\Delta x, \Delta y, \Delta z$ are corresponding orthogonal components of d with directions respectively the same as those defining v_R, v_T, v_N .

FIGURE 21 (Continued)

GEOMETRICAL RELATIONSHIPS AMONG THE EARTH AND
SATELLITES IN GEOSTATIONARY AND ECCENTRIC ORBITS

$$(5a) \Delta f_e = -\frac{f_o}{c} v_{SR} - \frac{f_1}{c} v_{SE}$$

$$(5b) \quad \approx -\frac{f_o}{c} v_{SR} - \frac{f_o}{c} v_{SE}$$

$$(5c) \quad \approx -\frac{f_o}{c} (v_R + v_{SE})$$

where v_{SE} is expressed by Equation 3. Substituting the expressions for v_R and v_T from Equation 4 into Equations 3 and 5 gives a numerical expression for Δf_e which is proportional to the eccentricity and is of the form:

$$(6a) \Delta f_e = -A \sin \left(\frac{2\pi}{T} t - \alpha \right)$$

where A is the maximum magnitude of Δf_e , and α is the numerical value of the phase of Δf_e with respect to that of v_R .

Let us denote A as Δf_{max} . Equation 6a can then be rewritten as:

$$(6b) \Delta f_e = -\Delta f_{max} \sin \frac{2\pi}{T} (t - t_o)$$

where $t_o = \frac{T}{2\pi} \alpha$. Irrespective of the location of P_E in the continental U.S.A., Δf_{max} has a value in the neighborhood of 50 Hz. The magnitude of t_o , which is the difference in time between when the radial velocity reaches its maximum and when Δf_e reaches its maximum, is less than half an hour. (The instantaneous frequency, f_e , at P_E is given by

$$f_e = f_o + \Delta f_e = f_o - \Delta f_{max} \sin \frac{2\pi}{T} (t - t_o).$$

This means that the power beam signal at P_E can be represented by a sinusoidally frequency modulated signal

$$v = V \sin\beta(t)$$

where

$$\beta(t) = \int (2\pi f_e) dt,$$

with a modulation period of 24 hours. Performing the indicated integration, with f_e obtained from Equation 7, yields

$$v = V \sin \left[2\pi f_o t + \Delta f_{\max} T \cos \frac{2\pi}{T} (t - t_o) + \beta_o \right]$$

where β_o is an arbitrary phase. (If f_o and Δf_{\max} are in Hertz, then t and T are in seconds.) The product $\Delta f_{\max} T$ is the modulation index, the ratio of the maximum frequency deviation, Δf_{\max} , to the modulating frequency, $1/T$.)

If t' is the time of day ($0 \leq t' \leq 24$ hours), then

$$(7) \quad t = t' - t_1$$

where t_1 is the time of day that the satellite is at its perigee. Combining Equations 7 and 6b provides the following form for Δf_e :

$$(8) \quad \Delta f_e = - \Delta f_{\max} \sin \frac{2\pi}{T} \left[t' - (t_o + t_1) \right].$$

Since the modulation index is very large, there is power at the following discrete frequencies at a given time of day, t' , from 60 satellites:

$$(9) \quad f_{en} = f_o - \Delta f_{\max_n} \sin \frac{2\pi}{T} \left[t' - (t_{on} + t_{1n}) \right]; \quad n = 1, 2, \dots, 60.$$

The t_{1n} are assumed to be statistically independent continuous random variables, each with a uniform probability density function given by

$$(10) p(t_{1n}) = \frac{1}{24}, \quad 0 \leq t_{1n} \leq 24.$$

In other words, any t_{1n} has equal probability of being any time during the day. Figure 2 is a plot of Equation 9 for a particular n , with $t' - (t_{on} + t_{1n})$ as the horizontal axis variable.

INSTANTANEOUS POWER SPECTRAL DISTRIBUTION

For equal power received from all satellites, the power in a frequency band at a given time of day is proportional to the number of spectral lines in that frequency band. The distribution of power in all bands forms a histogram, which when expressed on a percentage power basis, defines the Instantaneous Power Spectral Distribution, IPSD. This was depicted in Figure 5. Performing a time average of the IPSD's yields the Average Power Spectral Distribution (APSD). (It is sufficient to average over a period of 24 hours.)

MATHEMATICAL EXPRESSION FOR THE AVERAGE POWER SPECTRAL DISTRIBUTION

The APSD, expressed as a percentage distribution, is equivalently given by the expression

$$(11) \text{APSD}(f_i) = \frac{1}{60P} \sum_{n=1}^{60} \int_{f_i}^{f_i + \Delta f} S_n(f) df,$$

$i = \text{all integers from } 1 \text{ to } +\infty$

where $S_n(f)$ is the power spectral density of the signal received from satellite # n , P is the average power received from each of the 60 satellites, and f_i defines the frequency

bands, each band being Δf wide, where

$$(12) f_1 = i\Delta f.$$

The power spectral density of the signal received from a satellite with instantaneous frequency given by Equation 9 is, from Appendix B,

$$(13) S_n(f) = \begin{cases} \frac{1}{\pi} \frac{P_n}{\sqrt{\Delta f_{\max n}^2 - (f - f_0)^2}}; & |f - f_0| \leq \Delta f_{\max n} \\ 0; & |f - f_0| > \Delta f_{\max n} \end{cases}$$

where f_0 is the transmitted frequency of the pilot beam, and P_n is the average received power. Using Equation 13, the power in a band Δf wide at a frequency f_1 due the signal from satellite #n, with average power $P_n = P$, is:

$$(14) \int_{f_1}^{f_1 + \Delta f} S_n(f) df = \begin{cases} 0; & f_{i+1} - f_0 < -\Delta f_{\max n}, \text{ or } f_i - f_0 > \Delta f_{\max n} \\ \frac{P}{\pi} \left[\sin^{-1} \frac{f_{i+1} - f_0}{\Delta f_{\max n}} + \frac{\pi}{2} \right]; & f_i - f_0 \leq -\Delta f_{\max n}, \text{ and} \\ & f_{i+1} - f_0 > -\Delta f_{\max n} \\ \frac{P}{\pi} \left[\sin^{-1} \frac{f_{i+1} - f_0}{\Delta f_{\max n}} - \sin^{-1} \frac{f_i - f_0}{\Delta f_{\max n}} \right]; & |f_i - f_0| \leq \Delta f_{\max n} \\ & \text{and} \\ & |f_{i+1} - f_0| \leq \Delta f_{\max n} \\ \frac{P}{\pi} \left[\frac{\pi}{2} - \sin^{-1} \frac{f_i - f_0}{\Delta f_{\max n}} \right]; & f_{i+1} - f_0 \geq \Delta f_{\max n}, \text{ and} \\ & f_i - f_0 \leq \Delta f_{\max n} \end{cases}$$

where $f_{i+1} = f_i + \Delta f$.

Given Δf and the Δf_{\max_n} , Equation 11 for the APSD can then be numerically evaluated using Equations 12 and 14. Typical APSD's for two different Δf 's were shown in Figures 9 and 10.

MATHEMATICAL RELATIONSHIPS AMONG THE INSTANTANEOUS AND AVERAGE POWER SPECTRAL DISTRIBUTIONS AND THE POWER SPECTRAL DENSITY.

From Appendix C,

$$\text{IPSD}(f_i) = \frac{1}{60} \sum_{n=1}^{60} V(f_i - f_{en}),$$

$i = \text{all integers from } 1 \text{ to } +\infty$

where

$$V(f_i - f_{en}) = \begin{cases} 1 & \text{at } f_i \text{ for } f_i \leq f_{en} < f_i + \Delta f \\ 0, & \text{otherwise} \end{cases}$$

and where f_{en} is defined by Equation 9, and f_i defines the frequency bands, each band being Δf wide, where f_i is described by Equation 12. Thus, from Appendix C, it is proven that

$$\text{APSD}(f_i) = \frac{1}{24} \int_0^{24} \text{IPSD}(f_i) dt$$

is equivalent to Equation 11. Appendix C also develops the fact that

$$(15) \quad \text{APSD}(f_i) = E_{t_1} \{ \text{IPSD}(f_i) \}$$

where $E_{t_1} \{ \text{IPSD}(f_i) \}$ is the statistical expectation with respect to the times in the day when the satellites can be

at the perigees of their respective orbits.

Let $S(f)$ be the power spectral density due to the 60 satellites at a point of observation. Then,

$$(16) \quad S(f) = \sum_{n=1}^{60} S_n(f)$$

The average of $S(f)$ over a frequency interval, Δf , at a frequency f_i is given by

$$(17) \quad \overline{S(f_i)} = \frac{1}{\Delta f} \int_{f_i}^{f_i + \Delta f} S(f) df,$$

$i = \text{all integers from } 1 \text{ to } +\infty$

In terms of Equation 16 and 17, the APSD given by Equation 11 can then be expressed at a frequency, f_i , as:

$$(18) \quad \text{APSD}(f_i) = \frac{\Delta f}{60P} \overline{S(f_i)}.$$

As Δf approaches zero, $\overline{S(f_i)}$ approaches $S(f_i)$ in value, and thus

$$(19) \quad \lim_{\Delta f \rightarrow 0} \frac{\text{APSD}(f_i)}{\Delta f} = S(f_i)/60P$$

where f_i represents any frequency, and $S(f_i)/60P$ is the power spectral density, normalized in terms of total power. With the property given by Equation 19, the APSD, as expressed by Equation 18, can be thought of as a power-normalized, quantized version of the power spectral density.

BEAT FREQUENCIES

Two received satellite signals, $v_1(t)$ and $v_2(t)$, of equal amplitude (power) at slightly different instantaneous frequencies, f_1 and f_2 , give rise to a resulting composite signal of the form:

$$(20) \quad v_{12}(t) = E_{12}(t) \cos 2\pi f_{12} t$$

where

$$E_{12}(t) = 2V \cos 2\pi \left(\frac{f_1 - f_2}{2} \right) t,$$

$$f_{12} = \frac{f_1 + f_2}{2},$$

given that

$$v_{12}(t) = v_1(t) + v_2(t),$$

where

$$(21a) \quad v_1(t) = V \cos 2\pi f_1 t$$

and

$$(21b) \quad v_2(t) = V \cos 2\pi f_2 t.$$

The composite signal, $v_{12}(t)$ (Equation 20), and the amplitude function, $E_{12}(t)$, are shown in Figure 14. The frequency, f_{12} , is the geometric mean of f_1 and f_2 .

Beats, the maximum in amplitude of v_{12} , occur at a rate

$$2 \times \frac{|f_1 - f_2|}{2} = |f_1 - f_2|$$

since the maximums occur every half period of E_{12} as shown in Figure 14. We will only consider frequencies to be positive in value and since $f_1 - f_2$ may be negative, we will define the beat frequency to be

$$|f_1 - f_2|.$$

Beat frequency signals are formed by the product of two signals. For example, for $v_1(t)$ and $v_2(t)$ described by Equation 21:

$$\begin{aligned} v_1(t) \cdot v_2(t) &= V^2 \cos 2\pi f_1 t \cos 2\pi f_2 t \\ &= \frac{V^2}{2} \cos 2\pi(f_1 - f_2)t \\ &\quad + \frac{V^2}{2} \cos 2\pi(f_1 + f_2)t \end{aligned}$$

where $|(f_1 - f_2)|$ is the beat frequency.

For a square-law non-linear process,

$$[v_1(t) + v_2(t)]^2 = v_1^2(t) + 2v_1(t)v_2(t) + v_2^2(t),$$

and the beat frequency comes from the $v_1(t)v_2(t)$ term.

BEAT FREQUENCY EXPRESSION - SINUSOIDALLY VARYING FREQUENCIES

At a given time of day, t' , power received at a point of interest on earth from the 60 satellites is at the 60 sinusoidally varying frequencies given by Equation 9, and the beat frequency due to any two satellites which, is given by the magnitude of the difference in their frequencies, is:

$$|f_{ei} - f_{ej}| =$$

$$(22) \quad \left| \Delta f_{\max_1} \sin \frac{2\pi}{T} [t' - (t_{o1} + t_{1i})] \right.$$

$$\left. - \Delta f_{\max_j} \sin \frac{2\pi}{T} [t' - (t_{oj} + t_{1j})] \right|$$

where i and j refer to any two satellites, the " i th" and " j th" ones. Equation 22 yields an expression of the following form for the beat frequency:

$$(23) \quad F_{ij} \left| \sin \left(\frac{2\pi}{T} t' - \gamma_{ij} \right) \right|$$

where γ_{ij} is a phase term, and F_{ij} is the maximum value of the beat frequency. F_{ij} can have a value from $\left| \Delta f_{\max_1} - \Delta f_{\max_j} \right|$ when $(t_{o1} + t_{1i}) = (t_{oj} + t_{1j})$, i.e., when the variation in f_{ei} and f_{ej} are "in phase", to a value of $\left| \Delta f_{\max_1} + \Delta f_{\max_j} \right|$ when

$$(t_{o1} + t_{1i}) - (t_{oj} + t_{1j}) = 12 \text{ hours};$$

i.e., when the variation in f_{ei} and f_{ej} are "180° out of phase." This was alluded to in Figure 15.

DETERMINATION OF TOTAL NUMBER OF BEAT FREQUENCY SIGNALS

Sixty satellite signals yield

$$\frac{60!}{2!(60-2)!} = \frac{60(60-1)}{2} = 1770$$

possible beat frequency signals at any time. The satellite signal frequencies vary sinusoidally with time (Equation 9)

and the phases of these sinusoids ($\frac{2\pi}{T} t_{1n}$; $n = 1, 2, \dots, 60$) are random. Therefore, since the period of a beat frequency variation is 12 hours, there will be an infinite number of possible beat frequencies over a range from zero to approximately 100 Hz during a 12 hour period.

INSTANTANEOUS AND AVERAGE POWER SPECTRAL DISTRIBUTION OF BEAT FREQUENCY SIGNALS

For equal power received from all satellites, the $IPSD_B$ is (from Appendix D) expressed by

$$(24) \quad IPSD_B(f_i) = \frac{2}{60(60-1)} \sum_{n=1}^{60-1} \sum_{m=n+1}^{60} \nabla(f_i - |f_{em} - f_{en}|),$$

$i =$ all integers from 1 to $+\infty$

where

$$\nabla(f_i - |f_{em} - f_{en}|) = \begin{cases} 1 & \text{at } f_i \text{ for } f_i \leq |f_{em} - f_{en}| < f_i + \Delta f \\ 0, & \text{otherwise} \end{cases}$$

and where f_{em} and f_{en} are defined by Equation 9, and f_i defines the frequency bands, each band being Δf wide, where f_i is described by Equation 12.

Appendix D shows that Equation 24 is equivalent to the $IPSD_B$ obtained via self-correlation of the IPSPD:

$$(25) \quad IPSD_B(f_i) = \frac{2 \cdot 60}{60 - 1} \sum_{j=0}^{\infty} IPSD_B(f_j) IPSD_B(f_j - f_i),$$

$i =$ all integers from 1 to $+\infty$.

In general, Equation 25 is computationally simpler than Equation 24.

The $APSD_B$ is defined as the statistical expectation of the $IPSD_B$ with respect to the times in the day when the satellites can be at the perigees of their respective orbits:

$$(26) \quad APSD_B(f_1) = E_{t_1} \{IPSD_B(f_1)\}$$

$i =$ all integers from 1 to $+\infty$.

Appendix D shows that Equation 26 is equivalent to obtaining the $APSD_B$ via self-correlation of the $APSD$:

$$(27) \quad APSD_B(f_1) = \frac{2 \cdot 60}{60 - 1} \sum_{j=0}^{\infty} APSD(f_j) APSD(f_j - f_1),$$

$i =$ all integers from 1 to $+\infty$.

Also, from Appendix D, analogous to Equation 11,

$$(28) \quad APSD_B(f_1) \sim \int_{f_1}^{f_1 + \Delta f} S_B(f) df$$

where $S_B(f)$ is the power spectral density of the beat frequency signals and can be obtained from the self-correlation of the power spectral density, $S(f)$:

$$(29) \quad S_B(f) \sim \int_0^{\infty} S(f') S(f' - f) df'$$

where the power spectral density was defined in Equation 16.

MITIGATING STRATEGIES

1. Altering the Power Beam Transmit Frequency to Compensate for Frequency Shift at the Rectenna

Techniques that correct for the frequency shift at the Rectenna resulting from Doppler shifts by altering the transmit frequency of the power beam at the satellite all have the same corrected frequency shift at a point on earth. This is true whether direct or inferential ground measurement or phase conjugation with an on-board atomic clock is being used. The maximum magnitude of the corrected frequency shift is a function of the geographical location of that point. The governing equations are developed below.

a. Power Beam Frequency Shift Being Determined by Direct or Inferential Measurement.

To the expression for the uncompensated frequency shift of a power beam at a point, P_E , denoted as Δf_e , we add a correction term which is the amount that the power beam transmit frequency is altered and is equal to the negative of the Δf_e determined at the Rectenna. This yields the net or residual frequency shift in the power beam frequency at point P_E which we call the corrected frequency shift. Denoting the Δf_e determined at the Rectenna, as Δf_R , and $\Delta f'_e$ the corrected frequency shift at point P_E , we have

$$(30) \quad \Delta f'_e = \Delta f_e - \Delta f_R.$$

1.) Retrodirective Phase Control Being Employed

The uncompensated frequency shift, Δf_e , is given by Equation 5c:

$$\Delta f_e \cong - \frac{f_o}{c} (v_R + v_{SE}).$$

Therefore, since Δf_R is that Δf_e for the Rectenna,

$$\Delta f_R \cong - \frac{f_o}{c} (v_R + v_{SR}),$$

where v_{SR} is the v_{SE} pertaining to the Rectenna. Using the previously established fact that $v_{SR} \cong v_R$,

$$(31) \quad \Delta f_R \cong - \frac{2f_o}{c} v_R.$$

Substitution of the expressions for Δf_e and Δf_R from Equations 5c and 31 into Equation 30 yields

$$(32) \quad |\Delta f'_e| = \frac{f_o}{c} |v_R - v_{SE}|.$$

2.) Ground-Based Phase Control Being Employed.

The uncompensated frequency shift, Δf_e , is given by:

$$(33) \quad \Delta f_e = - \frac{f_o}{c} v_{SE}.$$

Therefore Δf_R , the Δf_e for the Rectenna, is given by:

$$(34) \quad \Delta f_R = - \frac{f_o}{c} v_{SR} = - \frac{f_o}{c} v_R.$$

Substitution of the expressions for Δf_e and Δf_R from Equations 33 and 34 into Equation 30 yields

$$|\Delta f'_e| = \frac{f_o}{c} |v_R - v_{SE}|,$$

which is identical to Equation 32.

b. Power Beam Frequency Shift Being Determined by Phase Conjugation with An On-Board Atomic Clock

Let Δf_o be the Doppler shift at the satellite of a signal transmitted from the Rectenna, referenced to the frequency, f_o , the desired frequency of the power beam at the Rectenna. At the satellite, the pilot beam frequency (retro-directive phase control) or the synthesized pilot frequency (ground based phase control) is then given by:

$$(35) f'_o = f_o + \Delta f_o.$$

As a result the phase conjugation of the signal at frequency, f'_o , with a conjugating signal at frequency $2f_o$, generated by an atomic clock, the power beam transmit frequency, f_1 , is

$$(36) f_1 = 2f_o - f'_o = f_o - \Delta f_o$$

Let Δf_1 be the Doppler shift in the power beam frequency at a point P_E , on earth. Therefore the power beam frequency at P_E is

$$(37) f_e = f_1 + \Delta f_1 = f_o - \Delta f_o + \Delta f_1$$

Now $\Delta f'_e$ is defined by the expression

$$\Delta f'_e = f_e - f_o.$$

Therefore

$$(38) |\Delta f'_e| = |f_e - f_o| = |\Delta f_1 - \Delta f_o|.$$

Now

$$(39) \Delta f_o = - \frac{f_o}{c} v_{SR} \approx - \frac{f_o}{c} v_{R'}$$

and

$$(40) \Delta f_1 = - \frac{f_1}{c} v_{SE} = - \frac{f_o}{c} v_{SE}$$

Substitution of the expressions for Δf_o and Δf_1 in Equations 39 and 40 into Equation 38 gives a result

$$|\Delta f'_e| = \frac{f_o}{c} |v_R - v_{SE}|,$$

identical to Equation 32 again.

c. Evaluation of the Maximum Magnitude of the Corrected Frequency Shift at a Point on Earth.

The corrected frequency shift magnitude, $|\Delta f'_e|$, expressed by Equation 32, has a maximum value, $|\Delta f'_e|_{\max}$ which can be evaluated by using Equation 3 to express v_{SE} , where v_R and v_T are given by Equation 4, and by using the fact that the maximum value of $(A \sin \Psi + B \cos \Psi)$ equals $\sqrt{A^2 + B^2}$, where A and B are arbitrary magnitudes, and Ψ is an arbitrary phase. The result, in Hertz, is:

$$|\Delta f'_e|_{\max} = 3.07 \frac{f_o}{c} \sqrt{\left[1 - \frac{\left(1 - \frac{r_E}{r_G} \cos \phi \cos \Delta \theta\right)}{\sqrt{1 + \left(\frac{r_E}{r_G}\right)^2 - 2 \frac{r_E}{r_G} \cos \phi \cos \Delta \theta}} \right]^2 + \left[\frac{2 \frac{r_E}{r_G} \cos \phi \sin \Delta \theta}{\sqrt{1 + \left(\frac{r_E}{r_G}\right)^2 - 2 \frac{r_E}{r_G} \cos \phi \cos \Delta \theta}} \right]^2}$$

where $f_o = 2.45 \times 10^9$ Hz, and $c = 3 \times 10^8$ m/s. Numerical solutions of Equation 41 for $0 \leq |\phi| < 90^\circ$ and $0 \leq |\Delta \theta| < 90^\circ$

yield the contours of Figure 20 when the power satellite is located above the equator at longitude 100° W. (The signal horizon in Figure 20, obtained from numerical solutions to Equation A-24 in Appendix A, assumes that the power beam signals do not propagate over the optical horizon of the earth as seen from a GEO satellite at longitude 100° W.) Generation of contours for power satellites located at other than longitude 100° W can be used in conjunction with Figure 20 to show that the maximum beat frequency possible in the continental U.S. for orbit eccentricities equal to 0.001 is about 9 Hz.

2. All Satellites Synchronized - Perturbations From GEO Identical At All Times

Two satellites which are in zero inclined orbits with eccentricities both equal to 0.001 and synchronized such that the magnitude and "phase" of their perturbations from GEO are identical at all times have identical relative positions at all times in orbits described by Figure 1. Therefore, for the two satellites, the velocities v_R and v_T given by Equation 4, which we denote here as v_{R1} , v_{R2} and v_{T1} , v_{T2} , will be respectively identical at all times, that is,

$$(42a) \quad v_{R1} \equiv v_{R2} \equiv v_R = 3.07 \sin \frac{2\pi}{T} t$$

$$(42b) \quad v_{T1} \equiv v_{T2} \equiv v_T = 6.13 \cos \frac{2\pi}{T} t$$

Referring to Equation 5c, if Δf_{e1} and Δf_{e2} are the respective Δf_e 's at a point, P_E , on earth due to the two satellites, then we can establish the relationships

$$\Delta f_{e1} = -\frac{f_o}{c} (v_{R1} + v_{SE1})$$

$$\Delta f_{e2} = -\frac{f_o}{c} (v_{R2} + v_{SE2}),$$

where v_{SE1} and v_{SE2} are the two v_{SE} 's at point P_E corresponding to the two satellites. Let f_{B12} be the beat frequency due to the two satellite power beams. Therefore,

$$(43) \quad f_{B12} = |\Delta f_{e1} - \Delta f_{e2}|.$$

Since $v_{R1} \equiv v_{R2}$ and $v_{T1} \equiv v_{T2}$,

$$(44) \quad f_{B12} = \frac{f_o}{c} |v_{SE1} - v_{SE2}|.$$

Equation 44 can be solved for the maximum value of f_{B12} (F_{12})^{*} using Equation 3 to express the v_{SE} 's, using the relationships given by Equation 42, and remembering that the maximum value of $(A \sin \Psi + B \cos \Psi)$ equals $\sqrt{A^2 + B^2}$, where A and B are arbitrary magnitudes, and Ψ is an arbitrary phase. The result, in Hertz, is:

*The maximum beat frequency is identical to F_{ij} in Equation 23 (for $i = 1, j = 2$).

(45)

$$F_{12} = 3.07 \frac{f_o}{c}$$

$$\left[\begin{aligned} & \frac{(1 - \frac{r_E}{r_G} \cos \phi \cos \Delta\theta_1)}{\sqrt{1 + (\frac{r_E}{r_G})^2 - 2 \frac{r_E}{r_G} \cos \phi \cos \Delta\theta_1}} \\ & - \frac{(1 - \frac{r_E}{r_G} \cos \phi \cos \Delta\theta_2)}{\sqrt{1 + (\frac{r_E}{r_G})^2 - 2 \frac{r_E}{r_G} \cos \phi \cos \Delta\theta_2}} \end{aligned} \right]^2 + 2^2 \left[\begin{aligned} & \frac{\frac{r_E}{r_G} \cos \phi \sin \Delta\theta_1}{\sqrt{1 + (\frac{r_E}{r_G})^2 - 2 \frac{r_E}{r_G} \cos \phi \cos \Delta\theta_1}} \\ & - \frac{\frac{r_E}{r_G} \cos \phi \sin \Delta\theta_2}{\sqrt{1 + (\frac{r_E}{r_G})^2 - 2 \frac{r_E}{r_G} \cos \phi \cos \Delta\theta_2}} \end{aligned} \right]^2$$

where $f_o = 2.45 \times 10^9$ Hz, $c = 3 \times 10^8$ m/sec, and where $\Delta\theta_1$ and $\Delta\theta_2$ are the $\Delta\theta$'s corresponding to the two satellites. Now F_{12} , here, is a function of ϕ , $\Delta\theta_1$, and $\Delta\theta_2$. Searching out the values of ϕ , $\Delta\theta_1$, and $\Delta\theta_2$ that maximize F_{12} yields

$$(46) \quad F_{12} < 5 \text{ Hz.}$$

Therefore, the maximum beat frequency is less than 5 Hz when all the satellites are in orbits with eccentricities equal to 0.001 and synchronized such that their perturbations from GEO are always identical.

ORIGINAL PAGE IS
OF POOR QUALITY

APPENDIX A

APPENDIX A

I. VELOCITY OF A SATELLITE IN AN ORBIT PERTURBED FROM GEO RELATIVE TO A POINT ON EARTH

a. Radial Velocity

Referring to Figure A-1, a satellite, whose orbit is perturbed from a geostationary orbit has a radial velocity, v , with respect to a point on earth, determined as follows. Let the rectangular coordinate system x_0, y_0, z_0 be such that the $x_0 - y_0$ plane is the equatorial plane, the North Pole lies on the $+z_0$ axis, and the Prime Meridian lies in the $x_0 - z_0$ plane. θ_E is then the longitude (East) of P_E , and $\phi = 90^\circ - \phi_E$ is its latitude (ϕ_E is the colatitude). The radius of the earth is r_E . If i_0, j_0, k_0 are unit vectors in the positive x_0, y_0, z_0 directions, respectively, then the location of P_E is defined by the vector, \vec{r}_E , where

$$(A-1) \quad \vec{r}_E = i_0 x_E + j_0 y_E + k_0 z_E$$

and

$$(A-2) \quad \begin{cases} x_E = r_E \sin \phi_E \cos \theta_E \\ y_E = r_E \sin \phi_E \sin \theta_E \\ z_E = r_E \cos \phi_E \end{cases}$$

PRECEDING PAGE BLANK NOT FILMED

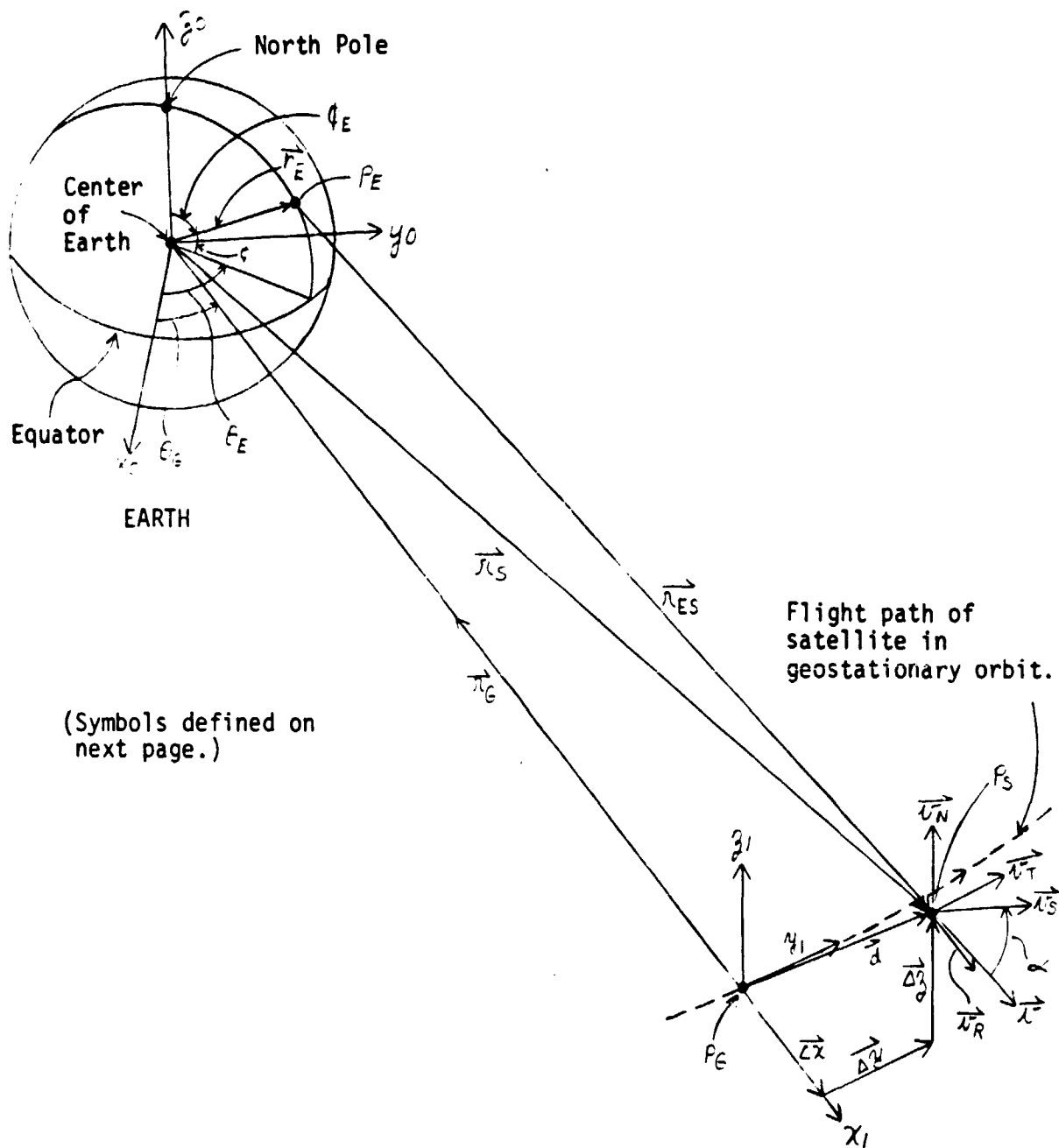


FIGURE A-1
 GEOMETRICAL RELATIONSHIPS BETWEEN THE EARTH AND
 A SATELLITE IN AN ORBIT PERTURBED FROM A GEOSTATIONARY ORBIT

DEFINITIONS OF SYMBOLS

- P_E = arbitrary point on the earth's surface
- P_S = instantaneous position of satellite relative to P_E
- P_G = mean position of satellite relative to P_E , equal to position of a satellite in geostationary orbit relative to P_E
- ϕ = latitude of P_E (positive in northern hemisphere, negative in southern)
- θ = colatitude of P_E
- θ_E = longitude of P_E (positive in eastern hemisphere, negative in western)
- θ_G = longitude of P_G (positive in eastern hemisphere, negative in western)
- v_S = instantaneous satellite velocity relative to P_G (and to P_E)
- $v_S = \sqrt{v_R^2 + v_T^2 + v_N^2}$, where v_R, v_T, v_N are corresponding orthogonal components of v_S with directions defined as follows:
- v_R : radially away from center of earth
- v_T : direction of flight path of geostationary satellite at P_G
- v_N : normal to equatorial plane (toward North Star)
- v = radial velocity of satellite with respect to P_E
- r_E = radius of earth
- r_G = radius of geostationary orbit
- r_S = vector from center of earth to P_S
- r_{ES} = vector from P_E to P_G
- α = angular difference in direction between satellite velocity and radial component of satellite velocity with respect to P_E
- d = distance between P_S and P_G (positional variation of P_S with respect to P_G)
- $d = \sqrt{(\Delta x)^2 + (\Delta y)^2 + (\Delta z)^2}$, where $\Delta x, \Delta y, \Delta z$ are corresponding orthogonal components of d with directions respectively the same as those defining v_R, v_T, v_N .

FIGURE A-1 (Continued)

GEOMETRICAL RELATIONSHIPS BETWEEN THE EARTH AND A SATELLITE IN AN ORBIT PERTURBED FROM A GEOSTATIONARY ORBIT

Let P_S be the instantaneous position of the satellite relative to P_E , with instantaneous velocity, v_S . If P_G , the mean position of the satellite relative to P_E , is the position of a satellite in geostationary orbit relative to P_E , then the vector, \vec{d} , which defines the deviation of the satellite from its mean location, represents the perturbation of P_S from geostationary orbit. For convenience, we define \vec{d} in the rectangular coordinate system x_1, y_1, z_1 centered on P_E . x_1 is in the direction of $-\vec{r}_G$, the negative of the vector from P_G to the center of the earth, and y_1 lies in the earth's equatorial plane. The magnitude of \vec{r}_G is the radius of the geostationary orbit. \vec{d} is made up of orthogonal component vectors $\vec{\Delta x}, \vec{\Delta y}, \vec{\Delta z}$ such that

$$\vec{d} = \vec{\Delta x} + \vec{\Delta y} + \vec{\Delta z}$$

If i_1, j_1, k_1 are unit vectors respectively in the positive x_1, y_1, z_1 directions, then

$$(A-3) \quad \vec{r}_G = -ir_G$$

and

$$(A-4) \quad \vec{d} = i_1 \Delta x + j_1 \Delta y + k_1 \Delta z$$

The radial velocity, \vec{v} , is the component of \vec{v}_S in the direction of \vec{r}_{ES} , the vector between P_E and P_S , and its magnitude is expressed by

$$(A-5) \quad v = v_S \cos \alpha.$$

Equation A-5 is obtained by taking the vector "dot" product,

$$(A-6) \quad v = \vec{v}_S \cdot \vec{e}_{ES},$$

where \vec{e}_{ES} is a unit vector in the direction of \vec{r}_{ES} . Therefore,

$$(A-7) \quad \vec{e}_S = \frac{\vec{r}_{ES}}{|\vec{r}_{ES}|}.$$

Substituting Equation A-7 into A-6 yields

$$(A-8) \quad v = \frac{\vec{v}_S \cdot \vec{r}_{ES}}{|\vec{r}_{ES}|}$$

If \vec{r}_S is a vector from the center of the earth to P_S , then

$$(A-9) \quad \vec{d} = \vec{r}_G + \vec{r}_S.$$

Now

$$(A-10) \quad \dot{\vec{r}}_S = \frac{d}{dt} (\vec{r}_S) = \vec{v}_S$$

Therefore,

$$\vec{v}_S = -\dot{\vec{r}}_G + \dot{\vec{d}},$$

which becomes, using Equations A-3 and A-4,

$$\vec{v}_S = -i_1 \dot{r}_G + i_1 \Delta \dot{x} + j_1 \Delta \dot{y} + k_1 \Delta \dot{y}.$$

But

$$\dot{r}_G = 0.$$

Therefore,

$$(A-11) \quad \vec{v}_S = i_1 \dot{\Delta x} + j_1 \dot{\Delta y} + k_1 \dot{\Delta z}.$$

Let

$$(A-12a) \quad \vec{v}_R \triangleq i_1 \dot{\Delta x}$$

$$(A-12b) \quad \vec{v}_T \triangleq j_1 \dot{\Delta y}$$

$$(A-12c) \quad \vec{v}_N \triangleq k_1 \dot{\Delta z}$$

Then Equation (A-11) becomes

$$(A-13) \quad \vec{v}_S = i_1 v_R + j_1 v_T + k_1 v_N.$$

(Note from Figure A-1 that v_N is the velocity component normal to the equatorial plane, and as Δx and Δy approach zero, relative to r_G , v_R and v_T respectively become the components of v_S radially away from the center of the earth and in the direction of the flight path of a satellite in geostationary orbit.)

Now

$$(A-14) \quad \vec{r}_{ES} = \vec{r}_S - \vec{r}_E$$

Using Equations A-1 through A-4 and Equation A-9, Equation A-14 becomes

$$(A-15) \quad \begin{aligned} \vec{r}_{ES} = & i_1 (r_G + \Delta x) + j_1 \Delta y + k_1 \Delta z \\ & - (i_0 r_E \sin \phi_E \cos \theta_E \\ & + j_0 r_E \sin \phi_E \sin \theta_E \\ & + k_0 r_E \cos \phi_E). \end{aligned}$$

Now it is seen that the unit vectors of the x_0, y_0, z_0 and x_1, y_1, z_1 coordinate systems are related as follows:

$$(A-16) \begin{cases} i_1 = i_0 \cos \theta_G + j_0 \sin \theta_G \\ j_1 = -i_0 \sin \theta_G + j_0 \cos \theta_G \\ k_1 = k_0 \end{cases}$$

Substituting the values for i_1, j_1, k_1 from Equation A-16 into Equations A-13 and A-15, performing the operations indicated in Equation A-8, and then letting $\phi = 90^\circ - \phi_0$ and

$$(A-17) \quad \Delta\theta = \theta_E - \theta_G$$

results in the following expression for v :

$$(A-18) \quad v = \frac{\begin{bmatrix} v_R [(r_G + \Delta x) - r_E \cos \phi \cos \Delta\theta] \\ + v_T [\Delta y - r_E \cos \phi \sin \Delta\theta] \\ + v_N [\Delta z - r_E \sin \phi] \end{bmatrix}}{\sqrt{\begin{aligned} &(r_G + \Delta x)^2 + \Delta y^2 + \Delta z^2 + r_E^2 \\ &- 2r_E \{ [(r_G + \Delta x) \cos \Delta\theta + \Delta y \sin \Delta\theta] \cos \phi \\ &\quad + \Delta z \sin \phi \} \end{aligned}}}$$

b. Relative Orbit Velocities v_R and v_T for Zero Inclination Orbit with Eccentricity = 0.001

The ellipse of Figure 1, as depicted in Figure 21, with parameters given by Figure A-1, is described by the equation

$$(A-19) \quad \left(\frac{\Delta x}{\Delta x_{\max}}\right)^2 + \left(\frac{\Delta y}{\Delta y_{\max}}\right)^2 = 1$$

where Δx_{\max} and Δy_{\max} are the maximum magnitudes of Δx and Δy .

By substitution into Equation A-19, it is easy to show that

$$(A-20a) \quad \Delta x = -\Delta x_{\max} \cos \frac{2\pi}{T} t$$

$$(A-20b) \quad \Delta y = \Delta y_{\max} \sin \frac{2\pi}{T} t$$

provide a solution to Equation A-19, where $T = 24$ hours, and t is the time, in hours, of the satellite from its perigee.

From Equation A-12,

$$v_R = \dot{\Delta x}$$

$$v_T = \dot{\Delta y}$$

Therefore, taking the time derivative of Equation A-20 yields

$$(A-21a) \quad v_R = \frac{2\pi}{T} \Delta x_{\max} \sin \frac{2\pi}{T} t$$

$$(A-21b) \quad v_T = \frac{2\pi}{T} \Delta y_{\max} \cos \frac{2\pi}{T} t.$$

The numerical values of Δx_{\max} and Δy_{\max} , which are found from inspection of Figure 1, are

$$\Delta x_{\max} = 42.164 \text{ km}$$

$$\Delta y_{\max} = 84.328 \text{ km.}$$

Note from Figure 1 that Δx_{\max} and Δy_{\max} are proportional to the orbital eccentricity. Thus v_R and v_T are proportional to orbital eccentricity. Since $T = 24$ hours = 24×3600 sec., Equation A-21 then becomes

$$(A-22a) \quad v_R = 3.07 \sin \frac{2\pi}{T} t \text{ (meters/sec.)}$$

$$(A-22b) \quad v_T = 6.13 \cos \frac{2\pi}{T} t \text{ (meters/sec.)}$$

II. OPTICAL HORIZON OF THE EARTH AS SEEN FROM A SATELLITE IN GEO

The optical horizon of the earth, as seen from a satellite in GEO, establishes the limit on the earth's surface over which a power beam is assumed not to propagate. An example is that shown in Figure 20. This horizon is the locus of points at which the vector \vec{r}_{ES} in Figure A-1 is 90° to the vector \vec{r}_E (with $\Delta x = \Delta y = \Delta z = 0$). In vector "dot" product notation, this relationship between \vec{r}_{ES} and \vec{r}_E can be expressed as

$$(A-23) \quad \vec{r}_E \cdot \vec{r}_{ES} = 0$$

where

$$\vec{r}_E \cdot \vec{r}_{ES} = r_E r_{ES} \cos \gamma$$

and $\gamma = 90^\circ$ is the angle between \vec{r}_E and \vec{r}_{ES} .

Using equations A-1, A-2, A-15, A-16, and A-17, Equation A-23 becomes (with $\Delta x = \Delta y = \Delta z = 0$ in Equation A-15):

$$(A-24) \quad \cos \phi \cos \theta = \frac{r_E}{r_G},$$

which yields the locus of points making up the horizon in terms of ϕ and $\Delta\theta$.

APPENDIX B
POWER SPECTRAL DENSITY OF A RECEIVED
SATELLITE POWER BEAM SIGNAL

APPENDIX B

POWER SPECTRAL DENSITY OF A RECEIVED SATELLITE POWER BEAM SIGNAL

Consider a power beam signal whose frequency varies according to Equation 9 which is repeated here for satellite #n, with $t' = (t_{on} + t_{ln})$ replaced by t_n'' :

$$(B-1) \quad f_{en} = f_o - \Delta f_{\max_n} \sin \frac{2\pi}{T} t_n''$$

(Since t' is the time of day, t_n'' varies from 0 to 24 during a $T = 24$ hour period.) Figure 2 is a plot of Equations 12 and B-1.

Now consider the energy received over a 24 hour period in a frequency band Δf Hz wide as shown in Figure B-1. If P_n is the average power in the received satellite signal, then, since the frequency is varying so slowly, all of that power is essentially received in the frequency band from f_a to $f_a + \Delta f$ during the time intervals from t_a to $t_a + \Delta t$ and from t_b to $t_b + \Delta t$. Thus the energy in the band at frequency f_a is represented mathematically as

$$(B-2) \quad E_n(f_a) \approx 2(P_n \Delta t)$$

But the energy in the frequency band is the power in the frequency spectrum from f_a to $f_a + \Delta f$ integrated over a

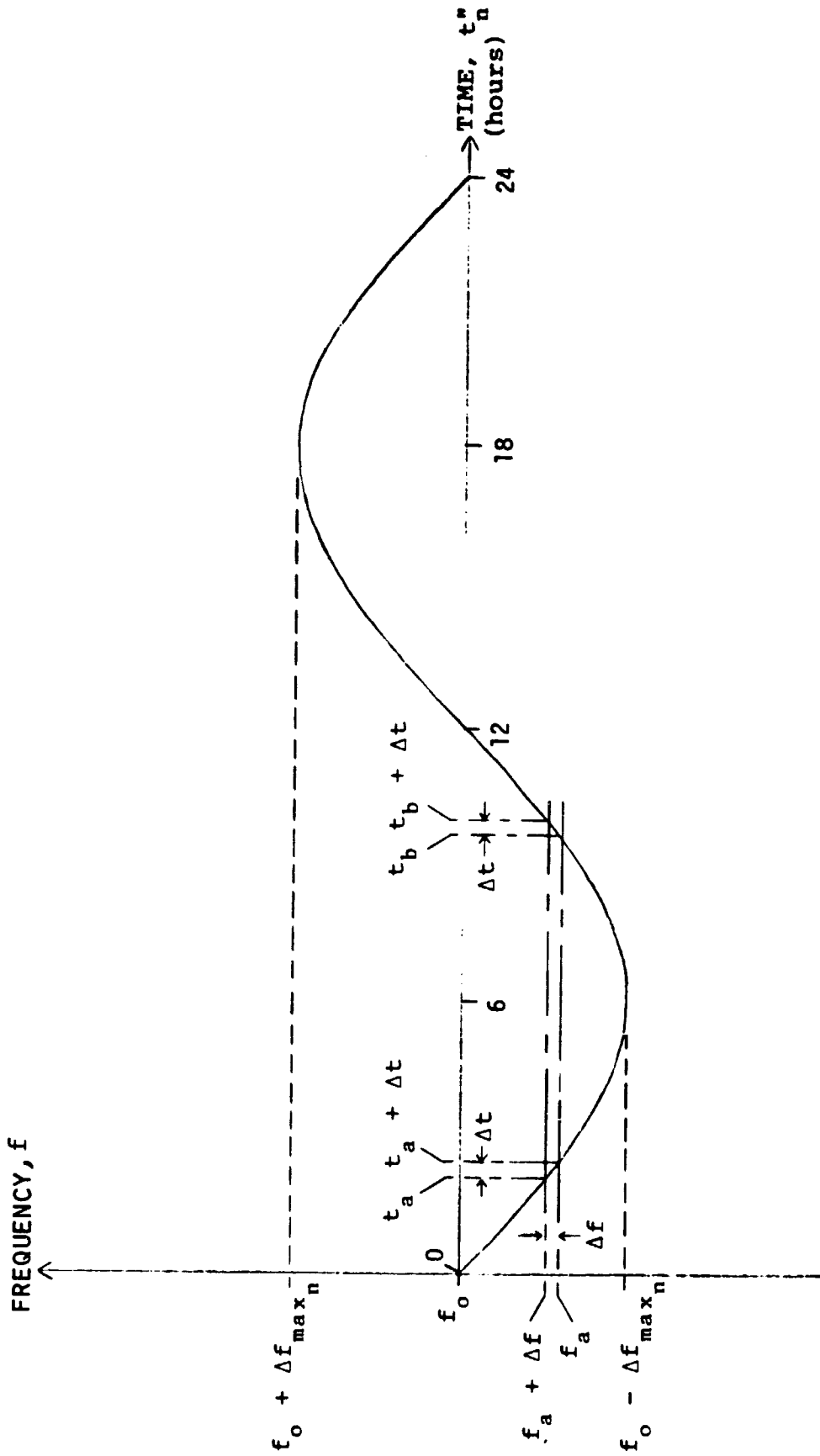


FIGURE B-1
 POWER BEAM FREQUENCY VARIATION DUE TO ECCENTRIC ORBIT
 -"DWELL TIME" IN A FREQUENCY BAND

24 hour period:

$$E_n(f_a) = \int_0^T \int_{f_a}^{f_a + \Delta f} S_n(f) df dt = T \int_{f_a}^{f_a + \Delta f} S_n(f) df$$

where $T = 24$ hours. Therefore,

$$T \int_{f_a}^{f_a + \Delta f} S_n(f) df \approx 2 P_n \Delta t$$

or

$$\frac{1}{\Delta f} \int_{f_a}^{f_a + \Delta f} S_n(f) df = \frac{2}{T} P_n \frac{\Delta t}{\Delta f} = \frac{2}{T} P_n \left| \frac{\Delta t}{\Delta f} \right|$$

As $\Delta f \rightarrow 0$,

$$(B-3) \quad \frac{1}{\Delta f} \int_{f_a}^{f_a + \Delta f} S_n(f) df \rightarrow S_n(f_a)$$

Now t_n'' can be considered to be a function of f_a so that

$$\frac{\Delta t}{\Delta f} = \left| \frac{t_n''(f_a + \Delta f) - t_n''(f_a)}{\Delta f} \right|$$

Therefore, as $\Delta f \rightarrow 0$,

$$(B-4) \quad \frac{2}{T} P_n \left| \frac{\Delta t}{\Delta f} \right| \rightarrow \frac{2}{T} P_n \left| \frac{dt_n''}{df_a} \right|$$

Since the frequency changes so slowly with time, Equation B-2 is still valid because even as the change in frequency, Δf , gets very small ($\Delta f \rightarrow 0$), the corresponding time interval, Δt , is still very large. Therefore we can equate Equations B-3 and B-4:

$$S_n(f_a) = \frac{2}{T} P_n \left| \frac{dt_n''}{df_a} \right|$$

Since f_a is an arbitrary frequency,

$$(B-5) \quad S_n(f) = \frac{2}{T} P_n \left| \frac{dt_n''}{df} \right|$$

From Equation B-1:

$$t_n'' = \frac{T}{2\pi} \sin^{-1} \frac{f_o - f_{en}}{f_{\max_n}}$$

Now f_{en} varies in frequency, f , from $f_o - f_{\max_n}$ to $f_o + \Delta f_{\max_n}$.

Therefore,

$$(B-6) \quad t_n'' = \frac{T}{2\pi} \sin^{-1} \frac{f_o - f}{\Delta f_{\max_n}}; \quad |f - f_o| \leq \Delta f_{\max_n}.$$

Performing the indicated derivative operation in Equation B-5 using the value of t_n'' and conditions on f from Equation B-6 yields the power spectral density:

$$(B-7) \quad S_n(f) = \begin{cases} \frac{1}{\pi} \frac{P_n}{\sqrt{\Delta f_{\max_n}^2 - (f - f_o)^2}}; & |f - f_o| \leq \Delta f_{\max_n} \\ 0; & |f - f_o| > \Delta f_{\max_n} \end{cases}$$

APPENDIX C

MATHEMATICAL DEVELOPMENT OF THE INSTANTANEOUS AND
AVERAGE POWER SPECTRAL DISTRIBUTION IN TERMS OF POWER
SPECTRAL DENSITY

APPENDIX C

MATHEMATICAL DEVELOPMENT OF THE INSTANTANEOUS AND AVERAGE POWER SPECTRAL DISTRIBUTIONS IN TERMS OF POWER SPECTRAL DENSITY

From Equation 9, the instantaneous frequency f_{en} , of the "n th" satellite's power beam signal as received at a point on earth is

$$f_{en} = f_o - \Delta f_{\max_n} \sin \frac{2\pi}{T} [t' - (t_{on} + t_{1n})]$$

where T is the time of day. Consider a period of time, about a specific time of day, t'_o , so that

$$(C-1) \quad t' - t'_o \ll T = 24 \text{ hours.}$$

Therefore the corresponding satellite power beam signal, v_n , as received at that point on earth is

$$(C-2) \quad v_n \approx V_n \cos [2\pi f_{en} (t' - t'_o) + \beta_n]$$

where

V_n = maximum signal amplitude

$$f_{en} = f_o - \Delta f_{\max_n} \sin \frac{2\pi}{T} [t'_o - (t_{on} + t_{1n})],$$

$$\approx f_o - \Delta f_{\max_n} \sin \frac{2\pi}{T} [t' - (t_{on} + t_{1n})],$$

β_n = arbitrary phase.

PRECEDING PAGE BLANK NOT FILMED

All of the β_n , ($n = 1, 2, 3 \dots N$), ($N = 60$ satellites), are considered to be uncorrelated (specifically, statistically independent) because the N satellite power beams are not phase locked together.

Now a sinusoid at a frequency f_r , with maximum amplitude, V , has its power spectral density, S , given by

$$S = \frac{V^2}{2} \delta(f - f_r)$$

where $V^2/2$ is the average power, and $\delta(f - f_r)$ is an impulse at $f = f_r$. Therefore the power spectral density, $\hat{S}(f)$, of N satellite power beam signals measured over a short period time at a specific time, t' , during the day is given by

$$(C-3) \quad \hat{S}(f) = \sum_{n=1}^N \hat{S}_n(f) \approx \sum_{n=1}^N P_n \delta(f - f_{en})$$

where P_n is the average power, $V_n^2/2$, of a signal. (If two or more f'_n are at the same frequency, we will consider $\hat{S}(f)$ to be the statistical expectation of the power spectral density at a time, t' , with respect to the phase, β_n . This means in this case that the powers are additive at a frequency because the β_n are uncorrelated. However, the percentage of time during a 24 hour period when two of the 60 sinusoidally varying frequencies are the same is, for all practical purposes, essentially zero).

We define the Instantaneous Power Spectral Distribution (IPSD) as

$$(C-4) \quad \text{IPSD}(f_i) = \frac{1}{\eta} \int_{f_i}^{f_i + \Delta f} \hat{S}(f) df,$$

$i = \text{all integers from } 1 \text{ to } \infty$

where η is the normalization factor so that

$$(C-5) \quad \sum_{i=1}^{\infty} \text{IPSD}(f_i) = 1 \text{ (100\%)}$$

where f_i defines the frequency bands, each band being Δf wide, where f_i is described by Equation 12. Substituting Equation C-4 into C-5, with $\hat{S}(f)$ in C-4 given by Equation C-3 and solving for η yields

$$\eta = \sum_{i=1}^{\infty} \int_{f_i}^{f_i + \Delta f} \left[\sum_{n=1}^N P_n \delta(f - f_{en}) \right] df$$

which becomes

$$\eta = \sum_{n=1}^N P_n \int_{f_1}^{\infty} \delta(f - f_{en}) df = \sum_{n=1}^N P_n$$

For this report, we assume that all P_n are the same power, P .
Therefore

$$\eta = NP$$

and

$$(C-6) \quad \text{IPSD}(f_i) = \frac{1}{N} \int_{f_i}^{f_i + \Delta f} \sum_{n=1}^N \delta(f - f_{en}) df.$$

Since

$$\int_{f_1}^{f_1 + \Delta f} \delta(f - f_{en}') df = \begin{cases} 1; & \text{if } f_1 \leq f_{en}' < f_1 + \Delta f, \\ 0; & \text{otherwise,} \end{cases}$$

the IPSD can also be expressed as

$$(C-7) \quad \text{IPSD}(f_1) = \frac{1}{N} \sum_{n=1}^N \nabla(f_1 - f_{en})$$

where

$$(C-8) \quad \Delta(f_1 - f_{en}) = \begin{cases} 1 @ f_1; & \text{for } f_1 \leq f_{en} < f_1 + \Delta f, \\ 0; & \text{otherwise.} \end{cases}$$

The twenty-four hour time average of the IPSD is the Average Power Spectral Density (APSD), and is given by the expression:

$$(C-9) \quad \text{APSD}(f_1) = \frac{1}{T} \int_0^T \text{IPSD}(f_1) dt'; \quad T = 24 \text{ hours.}$$

Substituting for $\text{IPSD}(f_1)$ from Equation C-6 yields:

$$\text{APSD}(f_1) = \frac{1}{T} \int_0^T \frac{1}{N} \int_{f_1}^{f_1 + \Delta f} \sum_{n=1}^N \delta(f - f_{en}') df dt'$$

$$(C-10) \quad \text{APSD}(f_1) = \frac{1}{NT} \sum_{n=1}^N \int_{f_1}^{f_1 + \Delta f} \left[\int_0^T \delta(f - f_{en}') dt' \right] df$$

Solving for t' from Equation 9, we see that t' can be thought of as a function of f_{en}' , that is,

$$t'(f_{en}) = \frac{T}{2\pi} \sin^{-1} \frac{f_0 - f_{en}}{\Delta f_{\max n}} + t_{on} + t_{ln}$$

Making a change in variables from time to frequency in the inner integral of Equation C-10 and taking the derivative of $t'(f_{en})$ with respect to f_{en} then yields

$$\begin{aligned} \int_0^T \delta(f - f_{en}) dt' &= \int_0^T \delta(f - f_{en}) |dt'| \\ &= \int_{f_{en}(0)}^{f_{en}(T)} \delta(f - f_{en}) \frac{T}{2\pi} \frac{1}{\sqrt{\Delta f_{\max n}^2 - (f_{en} - f_0)^2}} df_{en} \end{aligned}$$

where

$$f_{en}(0) = f_{en} \text{ when } t' = 0$$

and

$$f_{en}(T) = f_{en} \text{ when } t' = T.$$

But from Equation 13 we see that

$$\frac{1}{\pi} \frac{1}{\sqrt{\Delta f_{\max n}^2 - (f_{en} - f_0)^2}} = \frac{S_n(f_{en})}{P_n}$$

Therefore Equation C-10 becomes

$$\begin{aligned} \text{APSD}(f_1) &= \frac{1}{2N} \sum_{n=1}^N \frac{1}{P_n} \int_{f_1}^{f_1 + \Delta f} \\ \text{(C-11)} & \cdot \int_{f_{en}(0)}^{f_{en}(T)} \delta(f_{en} - f) S_n(f_{en}) dF_{en} df \end{aligned}$$

Now

$$(C-12) \int_{f_{en}(0)}^{f_{en}(t)} \delta(f_{en} - f) S_n(f_{en}) df_{en} = 2S_n(f),$$

because, as can be seen from Figure B-1, $f_{en} = f$, twice, for

$$f_n(0) \leq f_n(t') < f_n(T).$$

Substituting the results of Equation C-12 into C-11, and remembering that $P_n = P$ gives

$$(C-13) \text{APSD}(f_1) = \frac{1}{NP} \sum_{n=1}^N \int_{f_1}^{f_1 + \Delta f} S_n(f) df$$

But Equation C-13 is the same as Equation 11 ($N = 60$). Therefore, if the APSD is thought to be defined by Equation C-9, then we have just proved that Equation 11 is a valid equivalent definition. Note that Equation C-13 is equivalent to

$$(C-14) \text{APSD}(f_1) = \frac{1}{NP} \int_{f_1}^{f_1 + \Delta f} S(f) df$$

where

$$(C-15) S(f) = \sum_{n=1}^N S_n(f)$$

Note that imbedded within the inner integral in Equation C-10 is the fact that

$$(C-16a) S_n(f) = \frac{1}{T} \int_0^T \hat{S}_n(f) dt'$$

and

$$(C-16b) \quad S(f) = \frac{1}{T} \int_0^T \hat{S}(f) dt'$$

because, from Equation C-3, with $P_n = P$,

$$\hat{S}_n(f) \approx P \delta(f - f_{en}).$$

Now the statistical expectation of $S(f)$ with respect to the t_{1n} is given by

$$\begin{aligned} E_{t_1} \{ \hat{S}(f) \} &= \int_{-\infty}^{\infty} \dots \\ &\dots \int_{-\infty}^{\infty} \hat{S}(f) p(t_{11}, t_{12}, \dots, t_{1N}) dt_{11} dt_{12} \dots dt_{1N} \end{aligned}$$

Since the t_{1n} are statistically independent,

$$p(t_{11}, t_{12}, \dots, t_{1N}) = p(t_{11}) p(t_{12}) \dots p(t_{1N})$$

Using this fact and, from Equation 10, the fact that

$$p(t_{1n}) = 1/T, \quad 0 \leq t_{1n} < T, \quad \text{all } n,$$

yields:

$$(C-17a) \quad E_{t_1} \{ \hat{S}(f) \} = E_{t_1} \left\{ \sum_{n=1}^N \hat{S}_n(f) \right\}$$

$$(C-17b) \quad = \sum_{n=1}^N E_{t_1} \{ \hat{S}_n(f) \}$$

$$(C-17c) \quad = \sum_{n=1}^N \frac{1}{T} \int_0^T \hat{S}_n(f) dt_{1n}$$

$$(C-17d) \quad = \frac{1}{T} \int_0^T \hat{S}(f) dt_{1n}$$

because

$$(C-18) \quad \hat{S}_n(f) = P\delta(f - f_{en}(t_{1n}))$$

that is, $\hat{S}_n(f)$ is a function of only one of the t_{1n} , not of any other. From the form of Equation 9, we see that we can interchange t' and t_{1n} in the derivation subsequent to Equation C-10 to enable us to equate the appropriate expressions in Equation C-16 and C-17 to yield

$$(C-19a) \quad E_{t_1}\{\hat{S}_n(f)\} = S_n(f)$$

and

$$(C-19b) \quad E_{t_1}\{\hat{S}_n(f)\} = S_n(f)$$

Specifically, Equation C-19 says that the statistical expectation of the power spectral density at any time, t' , with respect to the time of day, t_{11} , t_{12} , etc, that the satellites can be at their perigees, is the same as a 24 hour time average of that power spectral density. This is tantamount to saying that the statistical expectation of the IPSD equals the APSD.

APPENDIX D

SPECTRAL DISTRIBUTION OF BEAT FREQUENCY SIGNALS

APPENDIX D

SPECTRAL DISTRIBUTION OF BEAT FREQUENCY SIGNALS

Beat frequency signals are formed by the product of two signals. The product of two signals results from square-law processing of the linear sum of two signals. Consider the square-law process which then has the input-output relationship

$$v_{out} = K v_{in}^2.$$

If v_{omn} symbolizes v_{out} when

$$v_{in} = v_m + v_n,$$

then

$$v_{omn} = K(v_m + v_n)^2.$$

When v_m and v_n are described by Equation C-2, with $t'' = t' - t_0 \ll T = 24 \text{ hours}$,

$$(D-1) \quad (v_m + v_n)^2 = v_m^2 + v_n^2 + 2v_m v_n = \begin{cases} 2V_n^2 + 2V_n^2 \cos [2\pi(2f_{en})t'' + 2\beta_n]; & m = n, \\ \left\{ \frac{V_m^2}{2} + \frac{V_m^2}{2} \cos [2\pi(2f_{en})t'' + 2\beta_m] \right. \\ \quad \left. + \frac{V_n^2}{2} + \frac{V_n^2}{2} \cos [2\pi(2f_{en})t'' + 2\beta_n] \right. \\ \quad \left. + (\text{continued on next page}) \right. \end{cases}$$

$$\begin{aligned}
 & + V_m V_n \cos \left[2\pi (f_{em} + f_{en}) t'' + (\beta_m + \beta_n) \right] \\
 \text{(D-1)} \quad & \text{cont'd.)} \\
 & + V_m V_n \cos \left[2\pi (f_{em} - f_{en}) t'' + (\beta_m - \beta_n) \right] \}; m \neq n.
 \end{aligned}$$

Only the last term in Equation D-1 is in the audio frequency range and is generally not at D.C. (zero frequency). It is generated by the product $v_m v_n$. This is the beat frequency signal due to two signals and is denoted here by v_{Bmn} , where v_{Bmn} is that portion of v_{omn} in the frequency region $|f_{em} - f_{en}|$, that is,

$$\text{(D-2)} \quad v_{Bmn} = KV_m V_n \left[2\pi (f_{em} - f_{en}) (t' - t_0) + (\beta_m - \beta_n) \right]; m \neq n.$$

Therefore the power spectral density, $\hat{S}_{Bmn}(f)$, of this beat frequency signal measured over a short period of time at a specific time, t'_0 , during the day is given by

$$\hat{S}_{Bmn}(f) = \frac{(KV_m V_n)^2}{2} \delta(f - (f_{em} - f_{en})); f > 0, m \neq n.$$

Let $\hat{S}_B(f)$ be the totality of the power spectral density of beat frequency signals from all $N = 60$ satellites around $t' = t'_0$. Therefore,

$$\text{(D-3)} \quad \hat{S}_B(f) = \sum_{m=1}^N \sum_{n=1}^N \hat{S}_{Bmn}(f), m \neq n.$$

Now

$$f_{en} - f_{em} = - (f_{em} - f_{en})$$

Therefore

$$\hat{S}_{Bnm}(f) = \frac{(KV V_n)^2}{2} \delta(f + (f_{em} - f_{en})); f > 0, m \neq n.$$

Suppose $f_{em} > f_{en}$. Then $\delta(f + (f_{em} - f_{en}))$ only has a value at $f = -(f_{em} - f_{en}) < 0$. But $f > 0$. Therefore $\hat{S}_{Bnm}(f) = 0$, and $\hat{S}_{Bmn}(f)$ is non-zero. Therefore, in general, either $\hat{S}_{Bnm}(f)$ or \hat{S}_{Bmn} will be zero, and Equation D-3 becomes

$$(D-4) \quad \hat{S}_B(f) = \sum_{m=1}^{N-1} \sum_{n=m+1}^N \frac{(KV V_n)^2}{2} \delta(f - |f_{en} - f_{em}|)$$

(If there are more than one beat frequency signals at a frequency, for example, $|f_{e9} - f_{e5}| = |f_{e7} - f_{e6}|$, then we will consider $\hat{S}_B(f)$ to be the statistical expectation of the power spectral density at time, t' , with respect to the phase β_n . This means that the powers are additive at that frequency because, as discussed in Appendix C, the β_n are uncorrelated.)

We define the Instantaneous Power Spectral Distribution of the beat frequency signals, $IPSD_B$, as

$$(D-5) \quad IPSD_B(f_i) \triangleq \frac{1}{\eta} \int_{f_i}^{f_i + \Delta f} \hat{S}_B(f) df;$$

$i = \text{all integers from } 1 \text{ to } +\infty,$

where η is a normalization factor so that

$$(D-6) \quad \sum_{i=1}^{\infty} \text{IPSD}_B(f_i) = 1 \quad (100\%)$$

Substituting Equation D-5 into D-6, with $\hat{S}_B(f)$ in Equation C-5 described by Equation D-4, and solving for η yields

$$\eta = 2K^2 \sum_{m=1}^{N-1} \sum_{n=m+1}^N P_m P_n$$

where

$$(D-7a) \quad P_m = \frac{V_m^2}{2}$$

and

$$(D-7b) \quad P_n = \frac{V_n^2}{2}$$

For this report, we assume that all P_n are the same power, P .

Therefore, P_m and P_n both equal P . Therefore,

$$\eta = 2(KP)^2 \frac{N(N-1)}{2} = (KP)^2 N(N-1)$$

and

$$(D-8) \quad \text{IPSD}_B(f_i) = \frac{2}{N(N-1)} \int_{f_i}^{f_i + f} \sum_{m=1}^{N-1} \sum_{n=m+1}^N \delta(f - |f_{em} - f_{en}|) df$$

Equation D-8 can also be expressed

$$(D-9) \quad \text{IPSD}_B(f_i) = \frac{2}{N(N-1)} \sum_{m=1}^{N-1} \sum_{n=m+1}^N \nabla(f_i - |f_{em} - f_{en}|)$$

where the ∇ function is defined in Equation C-8.

Now with $\text{IPSD}(f_1)$ given by Equation C-7, consider the self-correlation of $\text{IPSD}(f_1)$:

$$\begin{aligned}
 \text{IPSD}(f_1) * \text{IPSD}(f_1) &\triangleq \sum_{j=0}^{\infty} \text{IPSD}(f_j) \text{IPSD}(f_j - f_1) \\
 &= \sum_{j=0}^{\infty} \left[\frac{1}{N} \sum_{m=1}^N \nabla(f_j - f_{em}) \right] \left[\frac{1}{N} \sum_{n=1}^N \nabla(f_j - f_1 - f_{en}) \right] \\
 &= \frac{1}{N^2} \sum_{m=1}^N \sum_{n=1}^N \sum_{j=0}^{\infty} \nabla(f_j - f_{em}) \nabla(f_j - f_1 - f_{en}) \\
 &= \frac{1}{N^2} \sum_{m=1}^N \sum_{n=1}^N \nabla(f_{em} - f_1 - f_{en}) \\
 &= \frac{1}{N^2} \sum_{m=1}^N \sum_{n=1}^N \nabla(f_1 - (f_{em} - f_{en})),
 \end{aligned}$$

which yields

$$\begin{aligned}
 \text{IPSD}(f_1) * \text{IPSD}(f_1) &= \frac{1}{N^2} \sum_{m=1}^{N-1} \sum_{n=m+1}^N \nabla(f_1 - |f_{en} - f_{em}|) \\
 &\quad + \frac{1}{N^2} \sum_{m=1}^{N-1} \sum_{n=m+1}^N \nabla(f_1 + |f_{en} - f_{em}|) \\
 &\quad + \frac{1}{N^2} N \nabla(f_1)
 \end{aligned}$$

But $f_1 > 0$. Therefore,

$$(D-10) \quad \text{IPSD}(f_1) * \text{IPSD}(f_1) = \frac{1}{N^2} \sum_{m=1}^{N-1} \sum_{n=m+1}^N \nabla (f_1 - |f_{en} - f_{em}|).$$

Comparing Equation D-9 with D-10 gives

$$(D-11a) \quad \text{IPSD}_B(f_1) = \frac{2N}{N-1} \text{IPSD}(f_1) * \text{IPSD}(f_1)$$

$$(D-11b) \quad = \frac{2N}{N-1} \sum_{j=0}^{\infty} \text{IPSD}(f_j) \text{IPSD}(f_j - f_1);$$

$i = \text{all integers from } 1 \text{ to } +\infty.$

Thus, given the IPSD, it is a relatively simple matter to compute the IPSD_B .

We are interested in the Average Power Spectral Distribution of the beat frequency signals (APSD_B). But the average to be determined is the statistical average and not the time average. (It can be shown that $\frac{1}{T} \int_0^T \text{IPSD}(f_1) dt'$ does not necessarily equal $\text{APSD}_B(f_1)$.) Specifically, then, we want the statistical expectation of $\text{IPSD}_B(f_1)$ at any time of day, t' , with respect to the time of day, t_{11} , t_{12} , etc., that the satellites can be at their perigees. This is mathematically expressed as

$$(D-12) \quad \text{APSD}_B(f_1) = E_{t_1} \{ \text{IPSD}_B(f_1) \}.$$

Using Equation D-11, Equation D-12 becomes:

$$\text{APSD}_B(f_1) = E_{t_1} \left\{ \frac{2N}{N-1} \sum_{j=0}^{\infty} \text{IPSD}(f_j) \text{IPSD}(f_j - f_1); f_1 > 0. \right.$$

Using the expression for IPSD from Equation C-6 yields

$$\begin{aligned}
\text{APSD}_B(f_1) &= \frac{2N}{N-1} E_{t_1} \left\{ \sum_{j=0}^{\infty} \frac{1}{N} \int_{f_j}^{f_j + \Delta f} \sum_{m=1}^N \delta(f' - f_{em}) df' \right. \\
&\quad \cdot \left. \frac{1}{N} \int_{f_j - f_1}^{f_j - f_1 + \Delta f} \sum_{n=1}^N \delta(f'' - f_{en}) df'' \right\}; f_1 > 0, \\
&= \frac{2N}{N-1} \sum_{j=0}^{\infty} \int_{-\infty}^{\infty} \dots \int_{-\infty}^{\infty} \left[\frac{1}{N} \int_{f_1}^{f_j + \Delta f} \sum_{m=1}^N \delta(f' - f_{em}(t_{1m})) df' \right. \\
&\quad \cdot \left. \frac{1}{N} \int_{f_j - f_1}^{f_j - f_1 + \Delta f} \sum_{n=1}^N \delta(f'' - f_{en}(t_{1n})) df'' \right] p(t_{11}) \dots p(t_{1N}) dt_{11} \dots dt_{1N}; \\
&\quad f > 0.
\end{aligned}$$

Since from Equation 10, $p(t_{1n}) = 1/T$, $0 < t_{1n} < T$, all n ,

$$\begin{aligned}
\text{APSD}_B(f_1) &= \frac{2N}{N-1} \sum_{j=0}^{\infty} \left[\frac{1}{N} \sum_{\substack{m=1, \\ m \neq n}}^N \int_{f_j}^{f_j + \Delta f} \frac{1}{T} \int_0^T \delta(f' - f_{em}(t_{1m})) dt_{1m} df' \right. \\
\text{(D-13)} \quad &\quad \cdot \left. \frac{1}{N} \sum_{\substack{n=1, \\ m \neq n}}^N \int_{f_j - f_1}^{f_j - f_1 + \Delta f} \frac{1}{T} \int_0^T \delta(f'' - f_{en}(t_{1n})) dt_{1n} df'' \right] \\
&\quad f_1 > 0 \\
&\quad + \frac{2}{N(N-1)} \sum_{j=0}^{\infty} \sum_{n=1}^N \frac{1}{T} \int_0^T \int_{f_j}^{f_j + f_1 + \Delta f} \\
&\quad \cdot \int_{f_j - f_1}^{f_j - f_1 + \Delta f} \delta(f' - f_{en}) \delta(f'' - f_{en}) df'' df' dt_{1n}
\end{aligned}$$

The last term in Equation D-13 is the value of $\text{APSD}_B(f_1)$ when $m = n$ in the summation over m and n . In this term, the product $\delta(f' - f_{en}) \delta(f'' - f_{en})$ can only have a non-zero value when $f' = f'' = f_{en}$. But the range of f' is $f_j \leq f' < f_j + \Delta f$; that of f'' is $f_j - f_1 \leq f'' \leq f_j + \Delta f - f_1$, and the two ranges do not have any values in common unless $f_1 = 0$. However, $f_1 > 0$ in Equation D-13. Thus the last term in this equation is zero and we can drop the restriction $m \neq n$ on the other terms because $m = n$ produces a zero value. Using the results of Equations C-13, C-17b, C-17c, C-18, and C-19, $\text{APSD}_B(f_1)$ in Equation D-13 becomes

$$\begin{aligned}
 \text{APSD}_B(f_1) &= \frac{2N}{N-1} \sum_{j=0}^{\infty} \text{APSD}(f_j) \text{APSD}(f_j - f_1) \\
 \text{(D-14)} & \left. \begin{aligned} & \\ & = \frac{2N}{N-1} \text{APSD}(f_1) * \text{APSD}(f_1) \end{aligned} \right\} f_1 > 0
 \end{aligned}$$

Thus, given the $\text{APSD}(f_1)$, it is a relatively simple matter to compute the APSD_B via self-correlation of the APSD . (It is easy to show that the additional relationships below also hold:

$$\left. \begin{aligned}
 \hat{S}_B(f) &= 2K^2 \hat{S}(f) \hat{S}(f) \\
 &= 2K^2 \int_0^{\infty} \hat{S}(f') \hat{S}(f' - f) df'
 \end{aligned} \right\} f > 0$$

$$\begin{aligned}
 S_B(f) &= E_{t1} \{ \hat{S}_B(f) \} \\
 &= 2K^2 \int_0^{\infty} E_{t1} \{ \hat{S}(f') \} E_{t1} \{ \hat{S}(f' - f) \} df' \\
 &= 2K^2 \int_0^{\infty} S(f') S(f' - f) df'
 \end{aligned}
 \left. \vphantom{\begin{aligned} S_B(f) &= E_{t1} \{ \hat{S}_B(f) \} \\ &= 2K^2 \int_0^{\infty} E_{t1} \{ \hat{S}(f') \} E_{t1} \{ \hat{S}(f' - f) \} df' \\ &= 2K^2 \int_0^{\infty} S(f') S(f' - f) df' \right\} f > 0$$

$$\text{APSD}_B(f_1) = \frac{1}{N(N-1)(KP)^2} \int_{f_1}^{f_1 + \Delta f} S_B(f) df$$